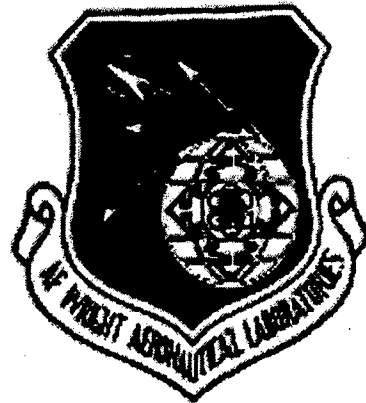


AFWAL-TM-80-68

**RANDOM VIBRATION TESTS
FOR PREDICTION OF FATIGUE
LIFE OF DIFFUSER STRUCTURE
FOR GAS DYNAMIC LASER**



**O. F. Maurer
D. L. Banaszak**

**Analytical Structural Mechanics Branch (AFRL/VASM)
Structures Division
Air Vehicles Directorate
Air Force Research Laboratory, Air Force Material Command
Wright-Patterson Air Force Base, OH 45433-7542**

JANUARY 1980

Final Report for 01 January 1979 – 01 December 1979

Approved for public release; distribution is unlimited.

20030123 053

**AIR VEHICLES DIRECTORATE
AIR FORCE RESEARCH LABORATORY
AIR FORCE MATERIEL COMMAND
WRIGHT-PATTERSON AIR FORCE BASE, OH 45433-7542**

NOTICE

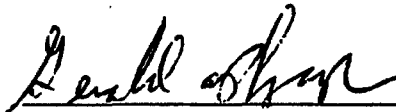
Using government drawings, specifications, or other data included in this document for any purpose other than government procurement does not in any way obligate the U.S. Government. The fact that the government formulated or supplied the drawings, specifications, or other data does not license the holder or any other person or corporation; or convey and rights or permission to manufacture, use, or sell any patented invention that may relate to them.

This report has been reviewed by the Office of Public Affairs (ASC/PA) and is releasable to the National Technical Information Service (NTIS). At NTIS, it will be available to the general public, including foreign nations.

This technical report has been reviewed and is approved for publication.



DAVID BANASZAK
Project Engineer
Analytical Structural Mechanics Branch
Structures Division



GERALD PLZAK
Technical Manager
Analytical Structural Mechanics Branch
Structures Division



JEROME PEARSON
Chief
Analytical Structural Mechanics Branch
Structures Division

Copies of this report should not be returned unless return is required by security considerations, contractual obligations, or notice on a specific document.

REPORT DOCUMENTATION PAGE

Form Approved
OMB No. 0704-0188

The public reporting burden for this collection of information is estimated to average 1 hour per response, including the time for reviewing instructions, searching existing data sources, gathering and maintaining the data needed, and completing and reviewing the collection of information. Send comments regarding this burden estimate or any other aspect of this collection of information, including suggestions for reducing this burden, to Department of Defense, Washington Headquarters Services, Directorate for Information Operations and Reports (0704-0188), 1215 Jefferson Davis Highway, Suite 1204, Arlington, VA 22202-4302. Respondents should be aware that notwithstanding any other provision of law, no person shall be subject to any penalty for failing to comply with a collection of information if it does not display a currently valid OMB control number. PLEASE DO NOT RETURN YOUR FORM TO THE ABOVE ADDRESS.

1. REPORT DATE (DD-MM-YY) January 1980			2. REPORT TYPE Final		3. DATES COVERED (From - To) 01/01/1979 - 12/01/1979	
4. TITLE AND SUBTITLE RANDOM VIBRATION TESTS FOR PREDICTION OF FATIGUE LIFE OF DIFFUSER STRUCTURE FOR GAS DYNAMIC LASER					5a. CONTRACT NUMBER IN-HOUSE	
					5b. GRANT NUMBER	
					5c. PROGRAM ELEMENT NUMBER N/A	
6. AUTHOR(S) O. F. Maurer D. L. Banaszak					5d. PROJECT NUMBER 317J	
					5e. TASK NUMBER 50	
					5f. WORK UNIT NUMBER 12	
7. PERFORMING ORGANIZATION NAME(S) AND ADDRESS(ES) Analytical Structural Mechanics Branch (AFRL/VASM) Structures Division Air Vehicles Directorate Air Force Research Laboratory, Air Force Materiel Command Wright-Patterson Air Force Base, OH 45433-7542					8. PERFORMING ORGANIZATION REPORT NUMBER AFWAL-TM-80-68-FBIG	
9. SPONSORING/MONITORING AGENCY NAME(S) AND ADDRESS(ES) Air Vehicles Directorate Air Force Research Laboratory Air Force Materiel Command Wright-Patterson Air Force Base, OH 45433-7542					10. SPONSORING/MONITORING AGENCY ACRONYM(S) AFRL/VASM	
					11. SPONSORING/MONITORING AGENCY REPORT NUMBER(S) AFWAL-TM-80-68	
12. DISTRIBUTION/AVAILABILITY STATEMENT Approved for public release; distribution is unlimited.						
13. SUPPLEMENTARY NOTES This is the best quality of the report available.						
14. ABSTRACT (Maximum 200 Words) Static and dynamic strain measurements which were taken during test stand operations of the gas dynamic laser (GDL) for the AF Airborne Laser Laboratory indicated that higher than expected vibrational stress levels may possibly limit the fatigue life of the laser structure. Particularly the diffuser sidewall structure exhibited large amplitude random vibrations which were excited by the internal gas flow. The diffuser structure consists of two layers of brazed stainless steel, AISI-347, panels. Cooling ducts were milled into the outer face sheet. These in turn are backed by the inner face sheet. So called T-rail stiffeners silverbrazed to the outer face sheets add the required stiffness and divide the sidewall into smaller rectangular plate sections.						
15. SUBJECT TERMS						
16. SECURITY CLASSIFICATION OF:			17. LIMITATION OF ABSTRACT: SAR	18. NUMBER OF PAGES 60	19a. NAME OF RESPONSIBLE PERSON (Monitor) David Banaszak	
a. REPORT Unclassified	b. ABSTRACT Unclassified	c. THIS PAGE Unclassified			19b. TELEPHONE NUMBER (Include Area Code) (937) 904-6859	

Standard Form 298 (Rev. 8-98)
Prescribed by ANSI Std. Z39-18

TABLE OF CONTENTS

INTRODUCTION	1
1. TEST DESCRIPTION	2
A. Test Articles	2
B. Test Instrumentation and Procedures	3
2. TEST RESULTS	6
A. Preliminary Experiments	6
B. Fatigue Results	9
3. APPLICATION OF RESULTS TO GDL DIFFUSER	10
A. Laser Test Data	10
B. Diffuser Fatigue Prediction	12
REFERENCES	14
TABLES	15
FIGURES	16

This document contains
blank pages that were
not filmed

LIST OF FIGURES

FIGURE	TITLE	PAGE
1	Typical Diffuser Sidewall Panel Details	16
2	Fatigue Test Article with Location of Straingage No. 4	17
3	Location of Straingages 1, 2, 3, on Testbeam	18
4	Test Setup for Fatigue Test	19
5	Shaker Control Setup	20
6	Strain Spectrum on Straingage No. 1, Beam #12, Before Failure	21
7	Strain Spectrum on Straingage No. 2, Beam #12, Before Failure	22
8	Strain Spectrum on Straingage No. 3, Beam #12, Before Failure	23
9	Strain Spectrum on Straingage No. 4., Beam #12, Before Failure	24
10	Strain Spectrum on Straingage No. 1, Beam #12, Immediately After Failure	25
11	Strain Spectrum on Straingage No. 1, Beam #12, After Crack Propagation to Inner Face Sheet	26
12	Strain Spectrum on Straingage No. 2, Beam #12, After Crack Propagation to Inner Face Sheet	27
13	Strain Spectrum on Straingage No. 3, Beam #12, After Crack Propagation to Inner Face Sheet	28
14	Resonant Frequency Reduction of Testbeam #6	29
15	Resonant Frequency Reduction of Testbeam #8	30
16	Resonant Frequency Reduction of Testbeam #9	31
17	Resonant Frequency Reduction of Testbeam #12	32
18	Test Article After Failure. Inner Face Sheet Undamaged	33
19	Testbeams with Lateral and Longitudinal Slots	34
20	Shaker Excitation Spectrum for Beam #12 Before Failure	35

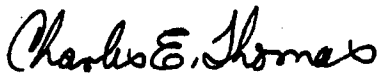
FIGURE	TITLE	PAGE
21	Shaker Excitation Spectrum for Beam #12 After Failure	36
22	Shaker Excitation Spectrum for Beam #12 After Crack Propagation Through Outer Face Sheet	37
23	Section of Strain Time History of Beam #2	38
24	Strain Peak Probability Density on Testbeam #12 Before Failure	39
25	Strain Peak Probability Density on Testbeam #12 After Failure	40
26	Strain Peak Probability Density on Testbeam #11 Before Failure	41
27	RMS Strain on Straingage #1 Versus Cycles To Failure	42
28	RMS Strain on Straingage #4 Versus Cycles To Failure	43
29	RMS Stress Versus Cycles to Failure as Measured on Straingage #1	44
30	RMS Stress Versus Cycles to Failure as Measured on Straingage #4	45
31	GDL Right Hand Stage, Inboard Diffuser Sidewall, Straingage Locations	46
32	Strain Spectrum on Straingage FSD 41 During GDL Run 111	47
33	Strain Time History of GDL Run 111 on Straingage FSD 41	48
34	Section of Strain Time History on Straingage FSD 41 During GDL Run 111	49

FOREWORD

This memorandum report documents an in-house effort conducted by the Structural Vibration Branch, Structures and Dynamics Division, Flight Dynamics Laboratory, Air Force Wright Aeronautical Laboratories, Wright-Patterson AFB, Ohio.

The effort was requested by the Air Force Weapons Laboratory and supported under Project Order Numbers 78-081 and 78-082. The work was performed under Job Order Number 317J5012. Mr Otto F. Maurer, AFWL/FIBGC, was the project engineer; Captain Charles Budde, AFWL/LRO, was the technical monitor.

This report has been reviewed and is approved.


CHARLES E THOMAS
Chief, Structural Vibration Branch
Structures and Dynamics Division

INTRODUCTION

Static and dynamic strain measurements which were taken during test stand operations of the gas dynamic laser (GDL) for the AF Airborne Laser Laboratory indicated that higher than expected vibrational stress levels may possibly limit the fatigue life of the laser structure. Particularly the diffuser sidewall structure exhibited large amplitude random vibrations which were excited by the internal gas flow. The diffuser structure consists of two layers of brazed stainless steel, AISI-347, panels. Cooling ducts were milled into the outer face sheet. These in turn are backed by the inner face sheet. So called T-rail stiffeners silverbrazed to the outer face sheets add the required stiffness and divide the sidewall into smaller rectangular plate sections. Details of a typical sidewall panel section are shown in Figure 1.

No vibrational random fatigue data were available for this type of structure. In addition the effect on the fatigue strength of the high temperature, experienced by the material during the brazing process, was not known. Therefore, it was decided that this information be obtained by random vibration fatigue tests of simple beam specimens which closely represented the panel construction and material. Due to the finite extension of the straingages and their inherent spatial averaging characteristic, the stress concentration effects near the stiffener attachment cannot be measured. However this approach permits a direct comparison of the measured dynamic strains at the diffuser and those of the testbeams, thus allowing predictions of the fatigue life of the diffuser sidewall.

This approach is widely used in the derivation of high cycle sonic fatigue data for stiffened aircraft structures. (Refs. 1 and 2). In this a beam with a stiffener section attached to the center is mounted on an

electro-dynamic shaker by clamping the web of the stiffener to the shaker table. It has been found (Ref 3) that in most cases the damage due to random vibration fatigue results from one predominant vibratory mode. Therefore, the bandwidth of the shaker random vibration is adjusted to cover several times the bandwidth of the fundamental or the second mode of the test article. The excitation bandwidth is usually centered near the modal frequency.

1. TEST DESCRIPTION

A. Test Articles

The test articles for the random vibration fatigue tests were designed to closely resemble a section of the diffuser sidewall panels and were manufactured by the identical process as was employed in the fabrication of the gas dynamic laser. The testbeam dimensions were selected as 10" x 3" x 0.125". The beam consisted of two layers of AISI-347 stainless steel silverbrazed together. Slots representing the cooling channels were machined into one of the two face sheets.

The dimensions of the beams were selected to give a fundamental frequency of approximately 200 Hz. A section of the T-rail stiffener was silverbrazed at the center to the milled layer as shown in Figure 2.

It was expected that a minimum of fifteen testbeams would be sufficient to derive the required fatigue data. Since it was not known whether the direction of the cooling channels or slots would influence the fatigue properties of the test articles, it was decided that in ten beams the direction would be longitudinal, while in the remaining five the channels would be directed across the width of the beam. In order to mount the test specimens on the specially designed shaker clamp, four bolt holes were drilled

into the web of the stiffener as shown in Figure 2.

Four straingages of the type BLH DLB-PT-12-2A with a gage factor of $3.34 \pm 2\%$ and a resistance of $118 \pm .5$ Ohms were bonded to the test articles. These gages were found to be highly fatigue resistant and very well suited for the intended purpose. For the number chosen and the location of the gages the following consideration prevailed:

The highest measurable strain was expected to exist on the top side directly over the edge of the stiffener flanges. Therefore the active element of Straingage No. 1 was placed in the longitudinal centerline over the edge of a stiffener flange as shown in Figure 3. Similarly Gage No. 2 was positioned over the opposite flange edge to one side of the beam. Straingage No. 3 was bonded to the center of the beam. Its main purpose was to monitor the beam stress if a delamination from the brazed stiffener should occur. Straingage No. 4 (Figure 2) was placed next to the edge of the braze-fillet in the longitudinal center-line. Its active element was 1/4 inch from the flange edge. Strain data from this gage were intended for comparison with the data measured on the diffuser sidewall.

B. Test Instrumentation and Procedures

A Ling (Calidyne) A-174 shaker system with a rated force output of 1500 lbs together with a Westinghouse C-20754, 10KW power supply was used as the driver in the fatigue tests. The control signal was obtained from a B&K 1042 sine-random generator, which fed through a GR1569 automatic level regulator into the control amplifier of the shaker.

A feedback signal was provided by an accelerometer which was attached to the mounting fixture of the shaker. The strain signals from the four straingages obtained at the AC coupled B&F 1-210A strain signal conditioners

and the shaker acceleration signal were fed through Intech amplifiers to the Honeywell 7400 magnetic tape recorders.

The strain signals as well as the acceleration signal were also available at a rms voltmeter, at an oscilloscope and at a Federal Scientific Ubiquitous real time spectrum analyzer. These instruments were used primarily to monitor the progress of the test and to set up and control the intended strain levels and spectra. A block diagram of the shaker power and control system as well as the data acquisition system is shown in Figure 4 and a picture of the complete test setup is given in Figure 5.

The natural frequency in the fundamental mode for all beams was experimentally determined by frequency sweeps using a HP frequency synthesizer as the control signal source. This was done at very low vibration levels in order not to accumulate any appreciable fatigue damage during these preliminary experiments.

Before each test and after every test interruption the straining channels and the acceleration channel were calibrated.

For the actual fatigue tests the random bandwidth of the B&K 1042 signal generator was set to 100 Hz centered at 180 Hz approximately 20 Hz below the fundamental resonant frequency of 200 Hz, for fourteen of the testbeams. Beam #15, which was in length 1 inch shorter than the others, exhibited a higher natural frequency of 248 Hz. The excitation bandwidth for this beam was centered at 220 Hz. The positioning of the excitation bandwidth was intended to permit the excitation of the test article at a constant level even if the beam natural frequency should drop by 70 Hz. A gradual reduction of the natural frequency is usually observed in such tests after an initial crack has developed and crack propagation is proceeding.

This fact was also used for determining the actual time to failure as will be explained later.

At the start of the test for each testbeam and after every test interruption, the magnitude of the excitation spectrum was adjusted to result in a desired nominal rms strain level at Straingage #1. Great care had to be exercised during this procedure and all monitoring instruments including the level regulator dial had to be consulted in order to obtain repetitive results. These instruments were observed continuously during the entire test duration, in order to notice any deviation from the set test conditions and to perform necessary readjustments.

Typical excitation spectra as measured by the accelerometer on the shaker table and typical strain spectra, obtained from the four straingages of a testbeam, are shown in Figures 20 through 22 and Figures 6 through 13.

During the test, immediately after the start or following any test interruption and approximately every 30 minutes thereafter, strain and acceleration signals were recorded for 30 seconds on a magnetic tape recorder for later data reduction and analysis.

For the purpose of determining the appearance of a crack, and to establish the time to failure of a test article, frequent checks of the testbeam were made. This required the removal of the test article from the clamping fixture and a subsequent treatment of suspected crack areas with dye penetrant. Failure was considered when a crack made visible by dye penetrant was noticed. This repetitive procedure was initially very time consuming. However, a close observation of the beam natural frequency indicated that a rapidly increasing reduction in the fundamental frequency closely correlated with the appearance of a visible crack. It was established that if a frequency rate of approximately -2 Hz per minute was reached

the test article had a crack. The elapsed time from the start of the test to reaching the -2Hz/min frequency rate was determined as the time to failure.

It appears from the test data that the higher dynamically loaded beams experienced a lower total drop in natural frequency until reaching the defined failure point (Beam #12 dropped 6 Hz) while the test specimens with the lower loading experienced a larger reduction of their natural frequency (Beam #9 dropped 14 Hz). Plots of natural frequency versus test time for several of the test articles are given in Figures 14 through 17. The number of cycles to failure was arrived at by numerical integration of the natural frequency $\nu(t)$ over the time to failure.

Most of the tests were continued after the failure point was reached until the specimen had attained a resonant frequency of 160 Hz to 140 Hz. In this range the crack which always originated at the edge of the stiffener flange, or the braze line close to the center of the beam, had propagated through the width and thickness of the milled or outer face sheet, while the top or inner face sheet still appeared undamaged (See Figure 18). Only two beams were tested to complete separation of the damaged section.

2. TEST RESULTS

A. Preliminary Experiments

Contrary to the initial expectation that noticeable differences should exist in the dynamic as well as in the fatigue characteristics of the two types of testbeams with the cooling ducts oriented in two orthogonal directions, longitudinal and lateral; no such differences could be observed. The first column of Table 1 shows the initial fundamental mode frequencies of the fifteen test articles. Testbeams #1 through #10 contain the slots in the longitudinal

direction, while in Testbeams #11 through #15 they are directed laterally. This is also shown in Figure 19.

It can be seen that the resonant frequencies of fourteen beams are very close to 200 Hz. Although Beams #11 and #12 indicate the highest resonant frequencies of 204 Hz and 205 Hz respectively, Beams #13 and #14, which are of the same type, are closer to the frequencies of the first ten test articles.

Beam #15, due to a manufacturing error, had the stiffener displaced by 1 inch off the center. Therefore, in order to obtain symmetry, one inch in length of one side had to be removed. This shorter test article had an initial resonant frequency of 248 Hz.

Damping coefficients which were determined for some of the testbeams indicated that damping ranged between 0.3% to 0.6%.

No reliable random fatigue data were obtained for Beam #1. The vibration level of the shaker for this beam was set up to generate a target rms strain level on Gage No. 1 near 1,000 $\mu\text{in/in}$. Within one to two minutes after test start the resonant frequency had dropped from 201 Hz to 150 Hz. A subsequent dye penetrant check revealed a crack near the flange edge. After continued testing for three hours, during which the excitation bandwidth, without change in level, was gradually moved with the changing resonant frequency down to 30 Hz, complete separation of the broken part was obtained. All subsequent tests were conducted at lower target rms strain levels.

It was also found during the initial tests that at high rms excitation levels the shaker mounting fixture experienced a feedback from the vibrating beam or a coupling between beam and fixture existed at the beam resonant frequency. This could not be eliminated by the available shaker control equipment which controlled to a constant force spectrum level. An acceleration

spectrum of the shaker head with Beam #12 during the fatigue test is shown in Figure 20. The following Figure 21 shows the shaker acceleration spectrum when the beam is near the defined failure point and the beam resonant frequency is at 190 Hz. Figure 22 shows the acceleration after the crack has propagated through the inner face sheet causing the beam resonant frequency to be near 140 Hz. The corresponding strain spectra on Gage No. 1 are shown in Figures 6, 10 and 11. From the six figures it can be seen that after the failure point has been reached the response level is gradually reduced and with it the feedback into the shaker acceleration. The strain spectra also show a gradual increase in the response bandwidth indicating increased damping or increasing nonlinear behaviour or both, as the crack propagates.

In order to further describe the behaviour of Beam 12, which is symptomatic for all other test articles, Figures 7 through 13 show the strain response spectra as obtained before and after failure on all straingages.

Figure 23 represents a section of the strain history as plotted from digitized data from Gage No. 1 before failure. The figure shows the typical narrowband random response expected from a single mode oscillation.

A plot of the probability density of positive and negative strain maxima, as obtained at Gage No. 1 before the failure point, is given in Figure 24. Also a Rayleigh probability density expected from an ideal narrow band response is given in the Figure. This indicates a slightly higher probability than expected by the Rayleigh distribution for strain peaks in the range between the 1.3σ and the 2.8σ level, while the probability for peaks below 1.3σ is reduced. Near the 3σ level the Rayleigh probability density is approached closely.

This general picture has been observed in previous random vibration fatigue tests (See for example, Ref 4). Figure 25, which shows the peak probability density during crack propagation after failure, indicates additional deviation from the theoretical distribution. Most of the other beams exhibited a peak distribution closer to that of Beam #11 which is shown in Figure 26. It approaches closely a Rayleigh distribution except for the very high peaks.

B. Fatigue Results

The number of cycles to the defined failure points and the rms strains as obtained on Gages No. 1 and No. 4 on fourteen of the test articles are tabulated in Table 1. It also lists the rms stresses which were calculated with a material modulus of elasticity $E = 2.8 \times 10^7$ psi. These data are plotted as strain or stress versus cycles to failure in Figures 27 through 30. The figures also present S-N curves which were obtained by least square fitting of a power function to the data. The scatter of the data was found to be within acceptable limits. This is borne out by the fact that the statistical correlation stayed between 0.97 and 0.98. The largest deviation was observed on Gage No. 1 of Testbeam #10. This may be attributed to a small gage misplacement. The plots further indicate that within the observed scatterband no noticeable difference exists between the two types of beams which were tested.

No delamination or failure of the brazing was observed. In all test articles the crack initiated in the surface of the outer face sheet close to the stiffener or brazeline edge, in or near the center of the beam. From here it propagated to the edge of the beam and through the thickness of the outer face sheet without immediate continuation into the inner face sheet.

Only after a significant increase in the test time the inner face sheet also developed a crack and the damaged beam section separated eventually. Complete separation was accomplished with only two test articles.

3. APPLICATION OF RESULTS TO GDL DIFFUSER

A. Laser Test Data

Measured data of GDL diffuser panel strains resulting from forty one test runs were reviewed. The data available were presented in various forms (rms strain or stress versus test time, strain or stress densities and strain or stress time-histories). It was found that three panel sections marked by the straingages FSD 41, FSD 39, FSD 21, showed the highest strains, with Gage FSD 41 located on Panel R9-C9 indicating consistently the highest values. The locations of these gages are shown in Figure 31.

Due to the type of test being conducted the strain levels in the different runs varied widely. It was determined that Runs #111, #113, and #299 produced the highest strains. At Straingage FSD 41 the peak rms strain level was 220 $\mu\text{in/in}$, in test Run #111, and 225 $\mu\text{in/in}$ in run 299.

A typical strain response spectrum obtained from Gage FSD 41 during Run #111 is given in Figure 32. The figure indicates essentially a single mode random response with a modal frequency near 800 Hz and a peak rms value of 220 $\mu\text{in/in}$. The complete time history of Run 111 is shown in Figure 33. A section of which, with a length of 40 milli-seconds has been expanded in Figure 34. This again strongly indicates an essentially narrow band or single degree of freedom random response with some superimposed noise.

Reviewing Figure 33 shows short transient conditions at the beginning and the end of the run. However the major part of the record appears to be stationary. It also can be seen that few peaks reach or exceed the 3σ level

of $3 \times 220 \mu\text{in/in}$. No peak probability density or a peak count was available for the record. However considering the section of 2.7 seconds of Figure 33, between 900 milliseconds and 3600 milliseconds and calculating an average number of peaks (negative or positive) by multiplication of the resonant frequency (800 Hz) with the time duration (2.7 secs), yields the average number of peaks to 2,160. A count of peaks, near the 3σ level indicates that less than 1% of the peaks is within the 3σ range. The Rayleigh peak probability density postulates that 3.3% of the peaks reach the 3σ level.

This cursory review seems to indicate the strain response peaks to be distributed slightly below a Rayleigh distribution at the high strain values. It may be remarked here, that if the response occurs essentially in one vibrational mode the distribution of peak amplitudes will closely follow a Rayleigh probability distribution. Added noise or contributions of weaker vibrational modes and small nonlinearities will modify the distribution to some extent, however the Rayleigh distribution in most cases will be a close approximation. It is therefore considered a reasonable assumption that the strain peaks in the diffuser panels during a near stationary run are distributed very similar to those resulting from the fatigue test.

Another consideration before application of the fatigue test results is the difference in strain measurements and the effect of the strain gradient at the measurement points. The active element of Gage FSD-41 was approximately 1/8 inch distant from the T-rail stiffener flange edge, while the filament of Gage No. 4 on a testbeam was 1/4 inch offset from the stiffener edge. Due to the steeper strain gradient in the panel near the edge, as compared to a testbeam, it can be expected that for equal strain indications on both straingages, the same stress will act at the fracture point, therefore the fatigue data as derived from Gage No. 4 on the testbeams can be directly applied.

B. Diffuser Fatigue Prediction

Under the assumption that the operational life of the diffuser consists of a series of statistically identical strain records similar to that given in Figure 33 with a constant rms value, the complete vibrational history can be considered stationary and ergodic.

Although previous experience with the test operation of the GDL indicated that the rms strain level varied widely in different runs, with Runs #111 and #299 indicating the highest values; the above assumption will result in a conservative prediction of the diffuser life.

In the following, the strain level resulting on Straingage FSD 41 during test run #299, will be used which shows a maximum rms strain of 225 $\mu\text{in/in}$ at a resonant frequency of 800 Hz. Applying this to the fitted fatigue curve of Figure 28 shows that with 225 $\mu\text{in/in}$ a life of 4.2×10^7 cycles can be obtained, which at a frequency of 800 Hz translates into 5.25×10^4 seconds or 14.6 hours. However in Figure 28 it can be seen that several measured failure points are below the average curve. Therefore in order to increase the confidence that failure will not occur prematurely, the data point farthest below the average curve will be included in the prediction by shifting the average fatigue curve through the data point occurring at 5.16×10^6 cycles and 262 $\mu\text{in/in}$ in Figure 28. With an expected maximum rms strain of 225 $\mu\text{in/in}$ on the diffuser panels an expected diffuser life of 1.4×10^7 cycles can be reached. This, in the absence of any static or thermal pre-stresses, translates into a fatigue life for the diffuser of 1.75×10^4 seconds or 4.86 hours, which in turn is 2,500 runs of seven seconds duration.

This fatigue life prediction contains basically three conservative assumptions:

1. The operation of the GDL generates rms stress levels over

the complete life at the maximum rms stresses observed up to date.-

2. The frequency of occurrence of high stress peak values is expected to follow closely a Rayleigh distribution which is approximated in the fatigue tests.

3. Inclusion of the lowest value of the scatterband for the measured fatigue data introduces additional confidence that no premature failure will occur.

It may be further remarked that the definition of failure, as the appearance of a crack made visible by dye penetrant, introduces an additional safety feature. As was mentioned earlier, the crack at this point had not propagated far into the depth and over the width of the test article. Additional time was required for the crack to reach the inner face sheet. This in practice means that the crack can be detected by leakage of cooling fluid in sufficient time before complete penetration through the panel.

REFERENCES

1. Ballentine, J. R., et al., "Refinement of Sonic Fatigue Structural Design Criteria," AFFDL-TR-67-156, 1968.
2. Rudder, E. F., Plumblee, H. E., "Sonic Fatigue Design Guide for Military Aircraft," AFFDL-TR-74-112, 1975.
3. Clarkson, B. L., "Stresses in Skin Panels Subjected to Random Acoustic Loading," Institute of Sound and Vibration - University of Southampton, May 1967.
4. Sandow, F., Jr., Maurer, O. F., "Random Vibration Fatigue Tests of Weldbonded and Bonded Joints," Shock and Vibration Bulletin, August 1976.

TABLE 1. SUMMARY OF TEST RESULTS

TEST BEAM NO.	INITIAL FUNDAMENTAL FREQUENCY HZ	N CYCLES TO FAILURE	STRAINAGE #1		STRAINAGE #4	
			S _{rms} psi	ε _{rms} μin/in	S _{rms} psi	ε _{rms} μin/in
1	202	No Data	No Data	No Data	No Data	No Data
2	200	4.8×10^4	2.086×10^4	745	1.663×10^4	594
3	201	1.69×10^6	1.211×10^4	432	1.019×10^4	364
4	201	1.41×10^7	0.918×10^4	328	0.767×10^4	274
5*	201	1.45×10^8	0.588×10^4	210	0.484×10^4	173
6	202	8.28×10^6	0.919×10^4	328	0.725×10^4	259
7	199	2.28×10^6	1.186×10^4	423	1.005×10^4	359
8	199	3.94×10^7	0.753×10^4	269	0.624×10^4	223
9	200	1.37×10^7	0.789×10^4	282	0.672×10^4	240
10	203	2.36×10^6	0.960×10^4	343	0.894×10^4	319
11	204	9.56×10^7	0.674×10^4	241	0.643×10^4	229
12	205	5.38×10^5	1.431×10^4	511	1.195×10^4	427
13	200	7.16×10^6	0.946×10^4	338	0.823×10^4	294
14	202	5.16×10^6	0.896×10^4	320	0.735×10^4	262
15	248	2.75×10^7	0.815×10^4	291	0.690×10^4	246

* Not Failed

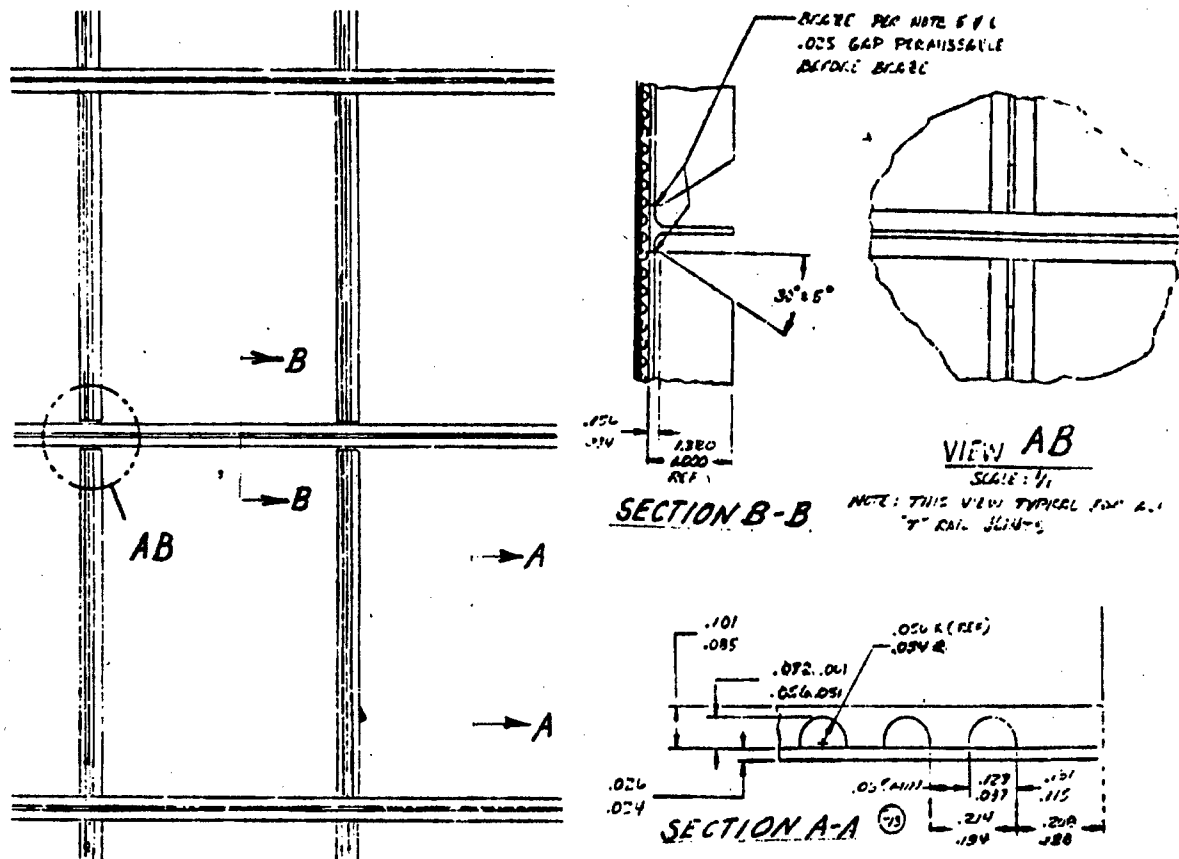


Figure 1. Typical Diffuser Sidewall Panel Details.

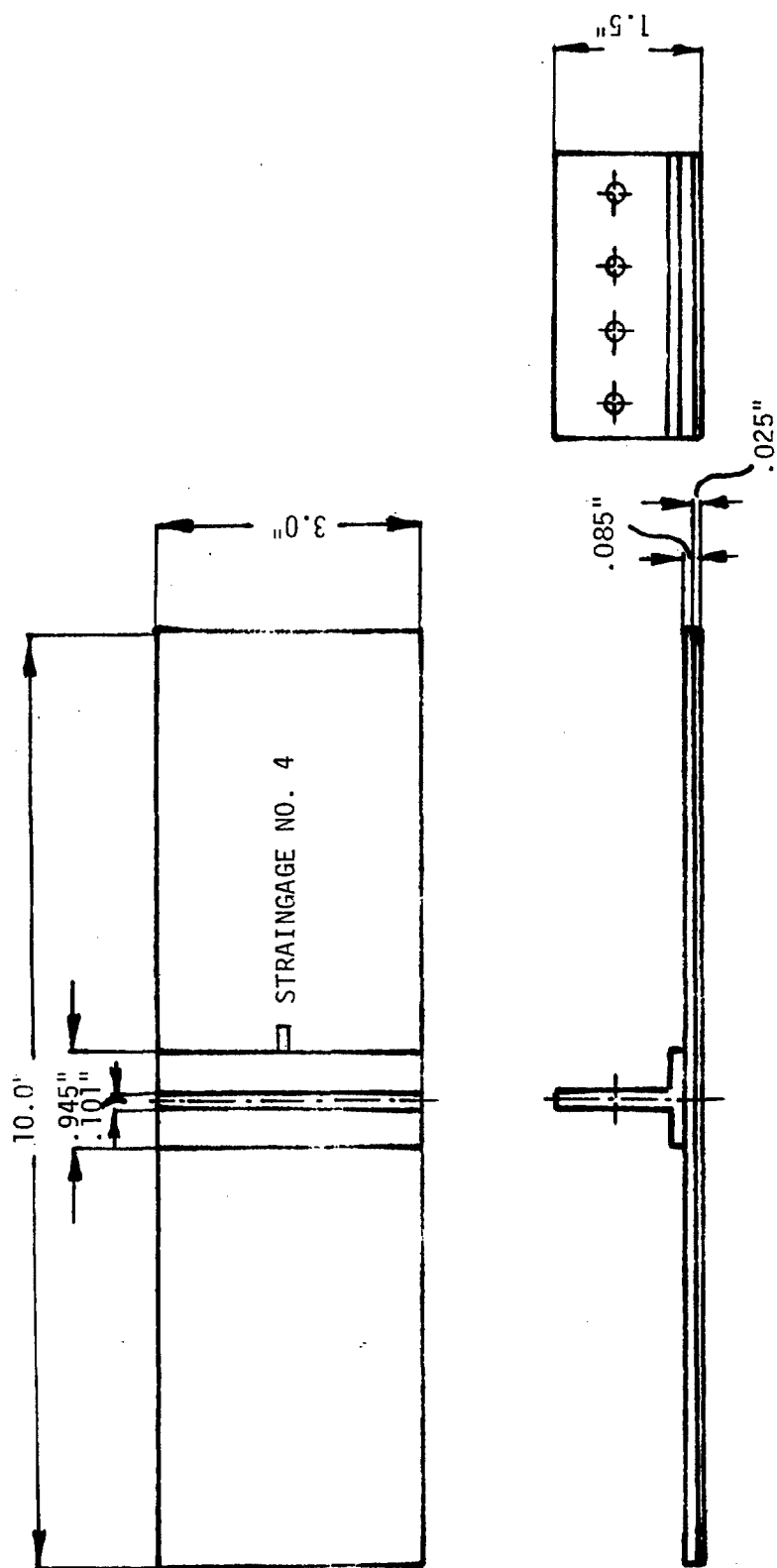


Figure 2. Fatigue Test Article with Location of Strainage No. 4.

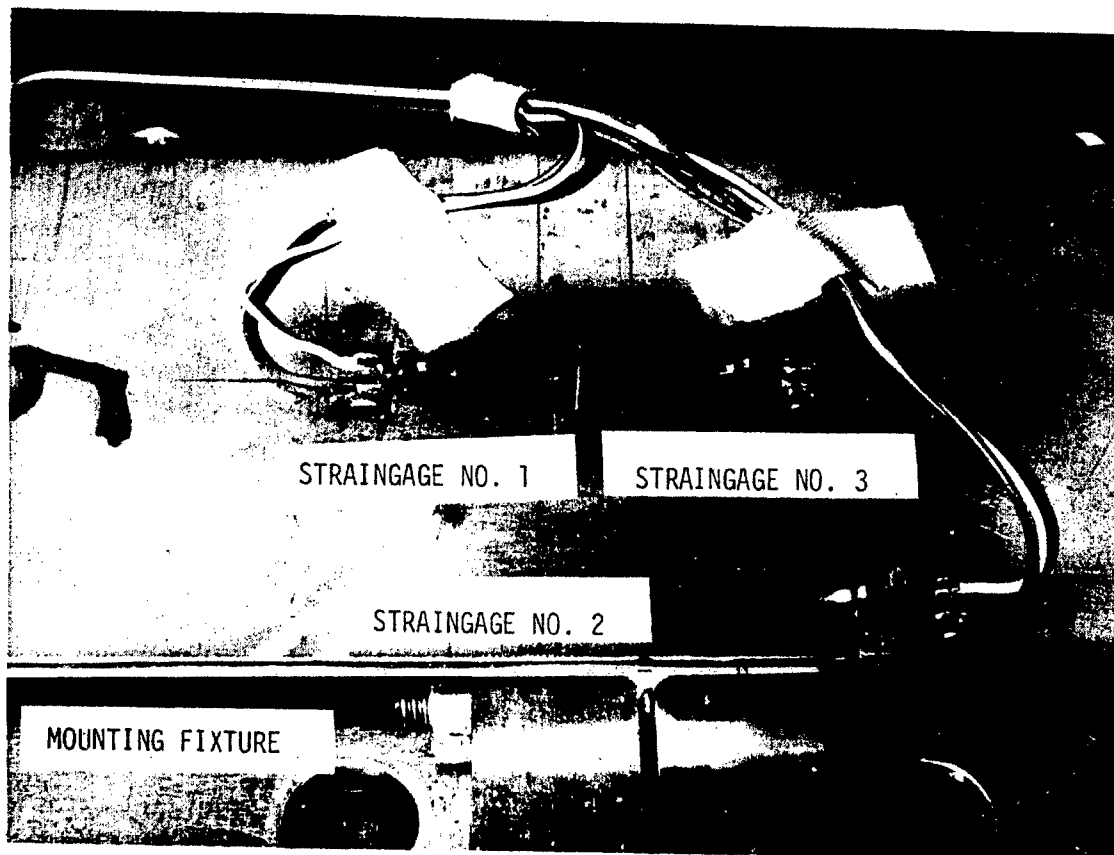


Figure 3. Location of Straingages 1, 2, 3, on Testbeam.

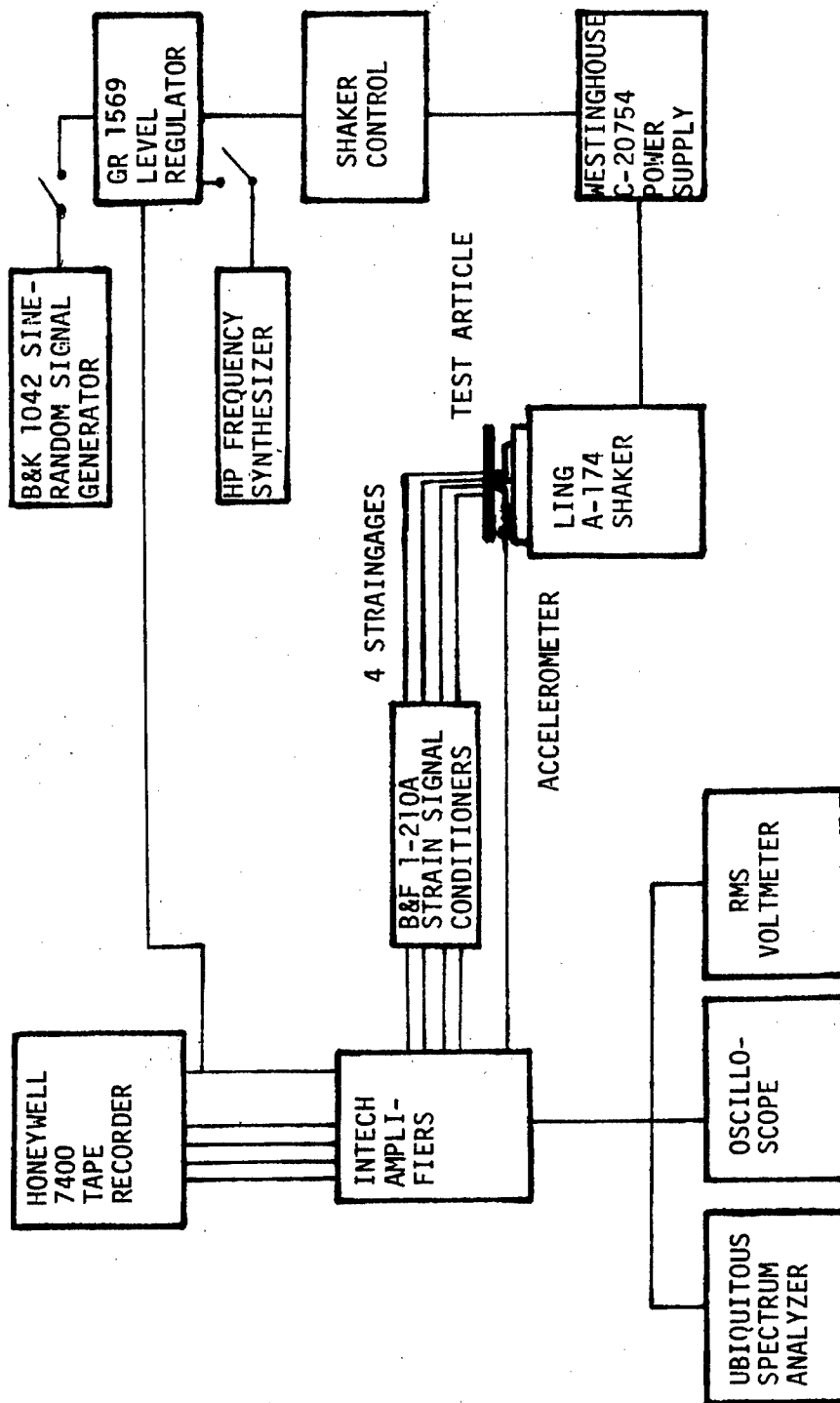


Figure 4. Test Setup for Fatigue Test.

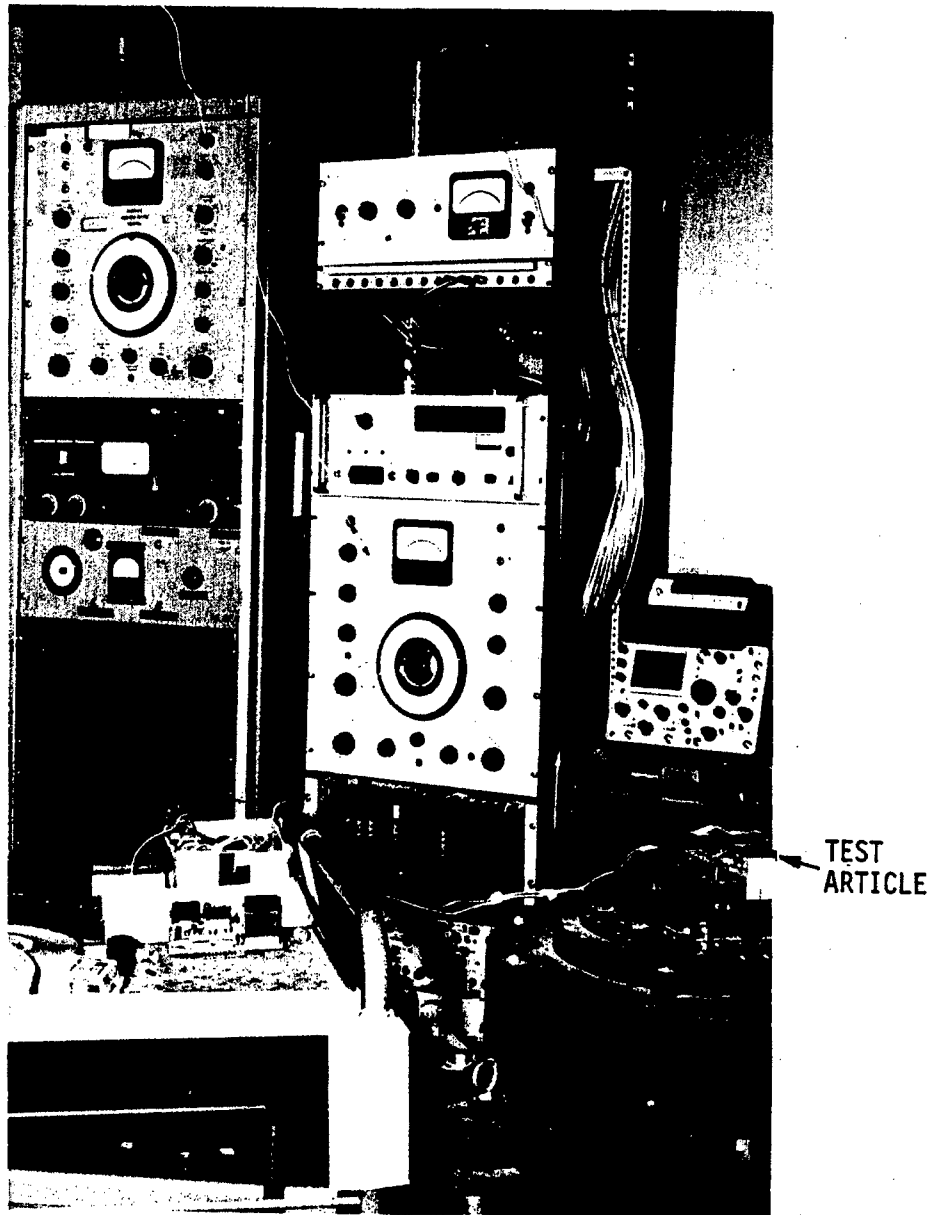


Figure 5. Shaker Control Setup.

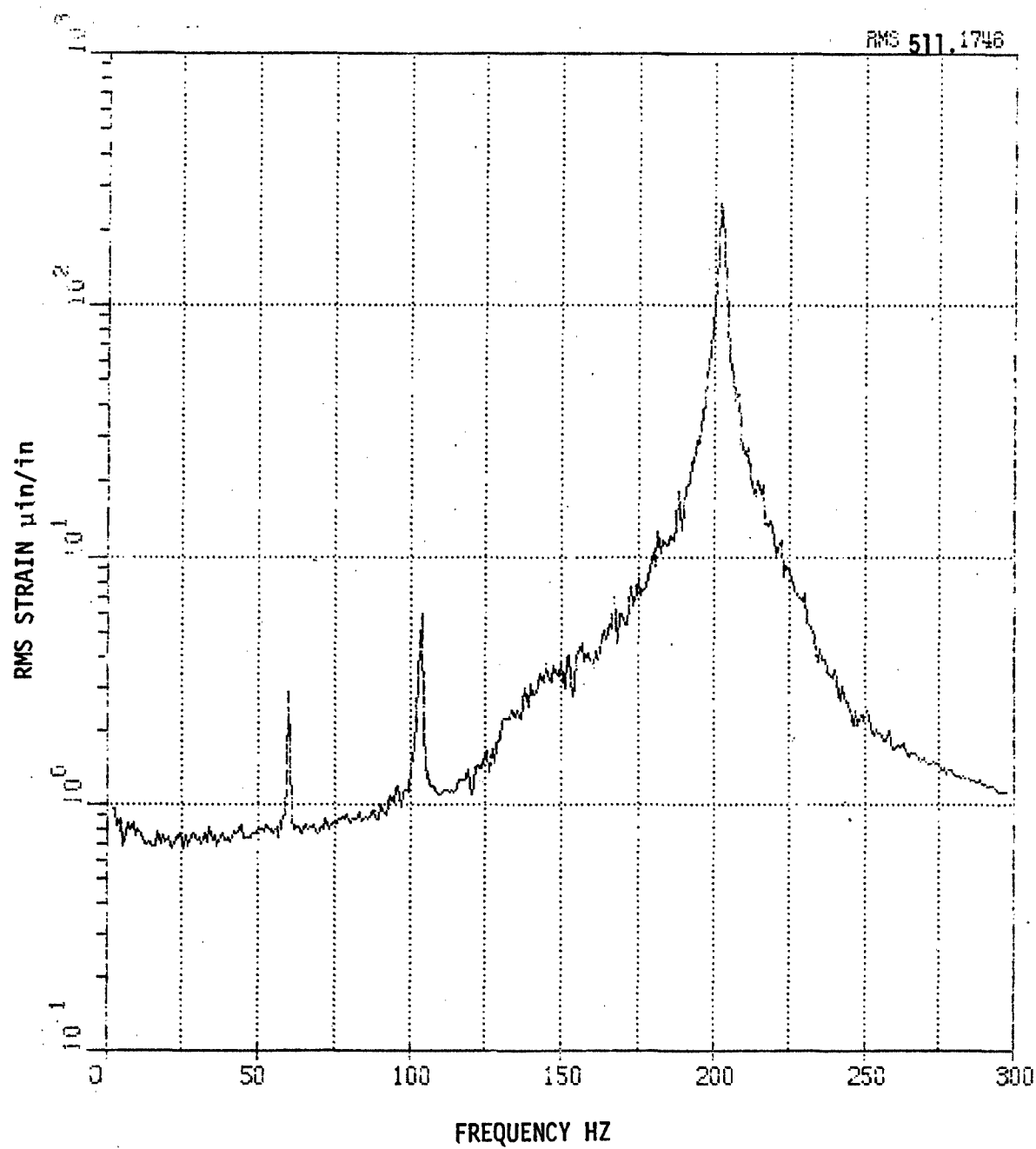


Figure 6. Strain Spectrum on Straingage No. 1, Beam #12, Before Failure.

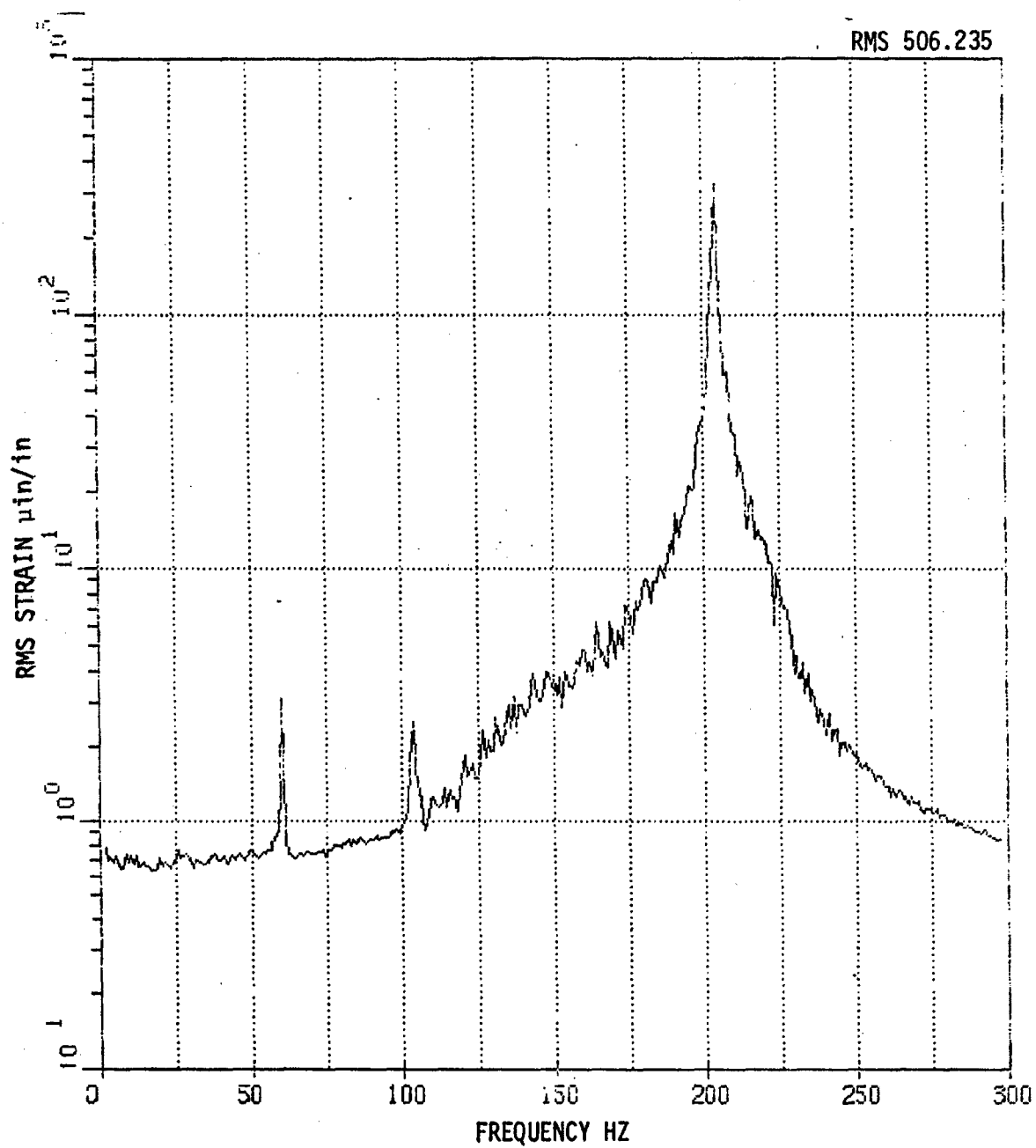


Figure 7. Strain Spectrum on Straingage No. 2, Beam #12, Before Failure.

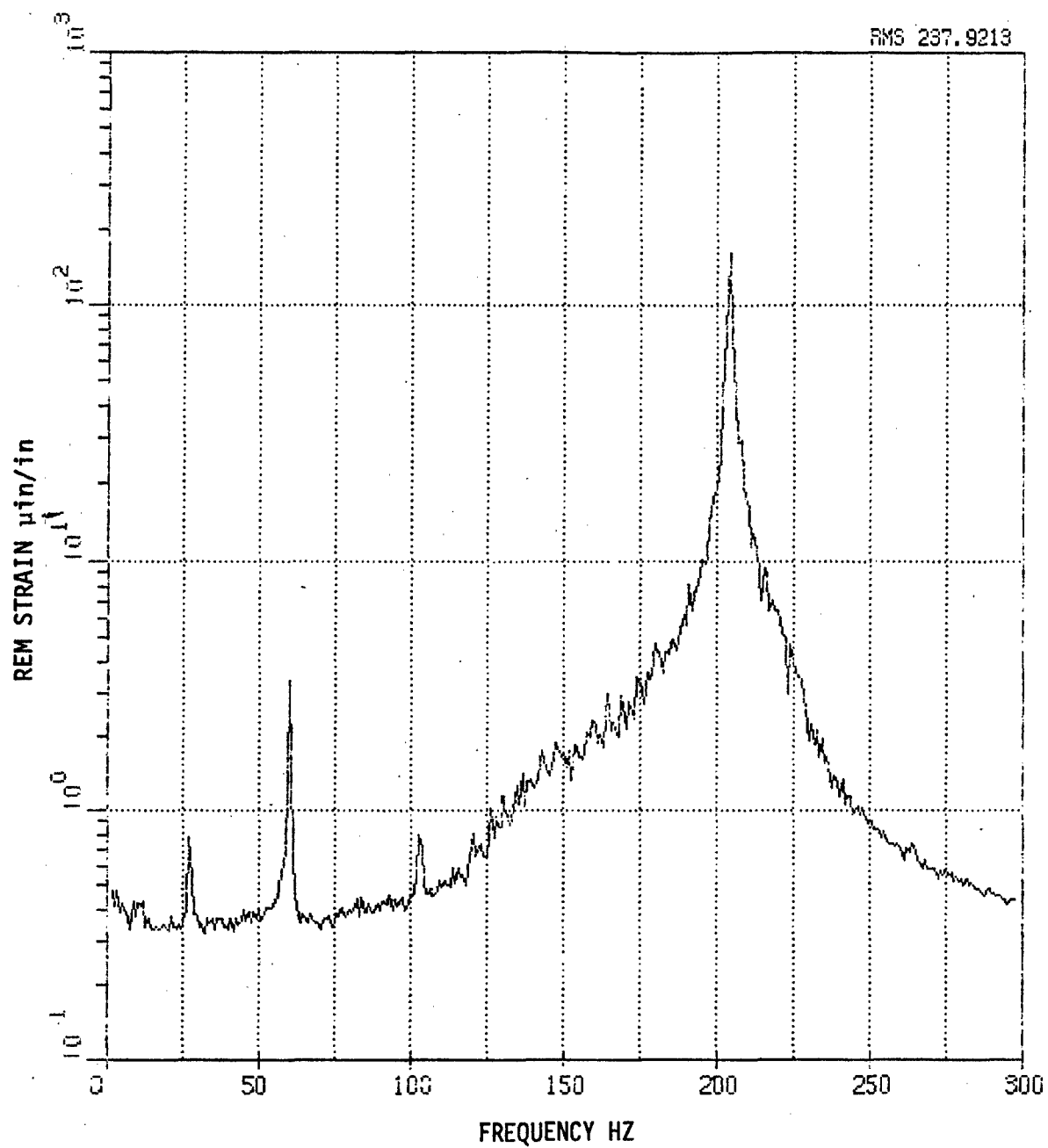


Figure 8. Strain Spectrum on Straingage No. 3, Beam #12, Before Failure.

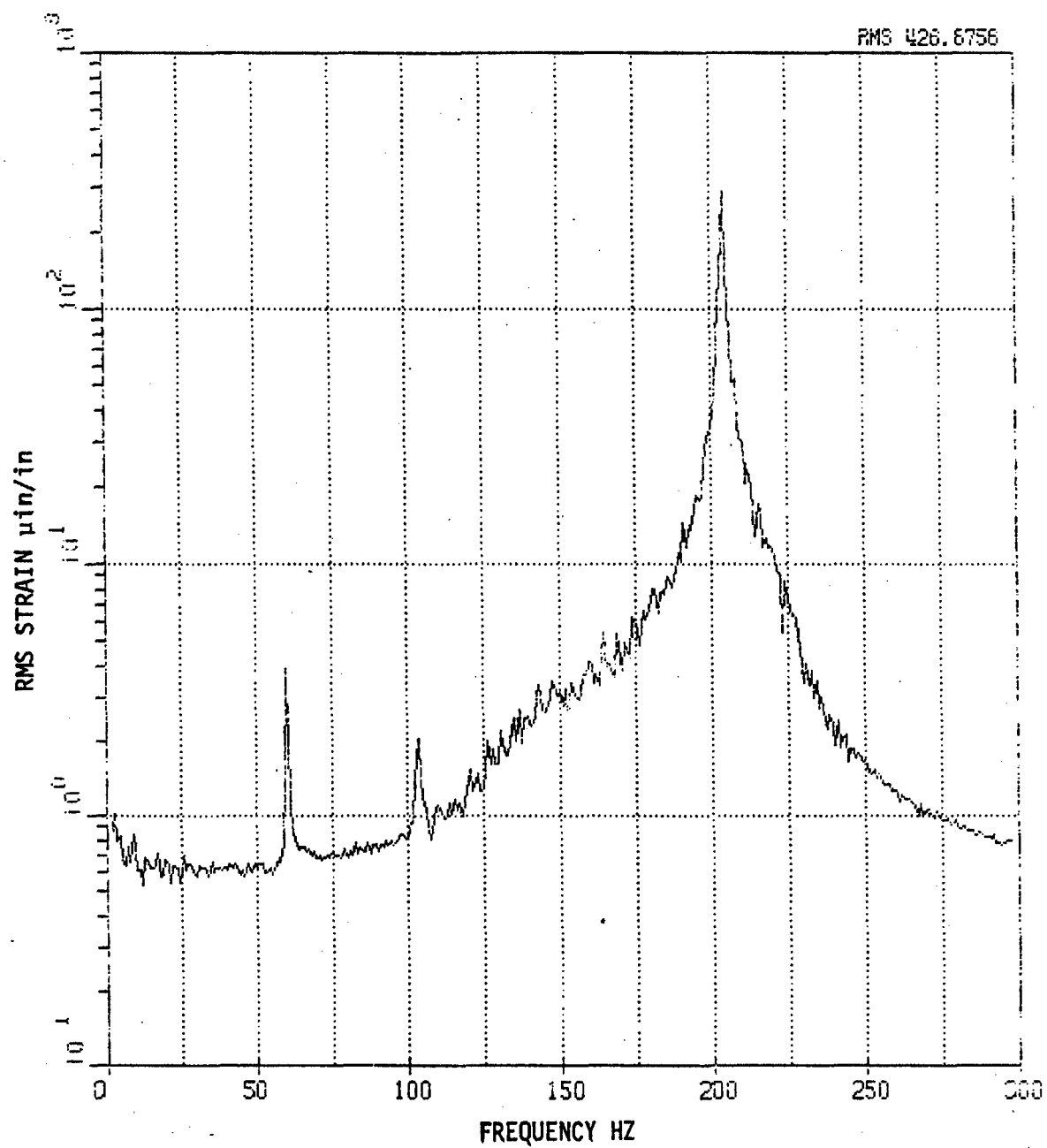


Figure 9. Strain Spectrum on Straingage No. 4, Beam #12, Before Failure.

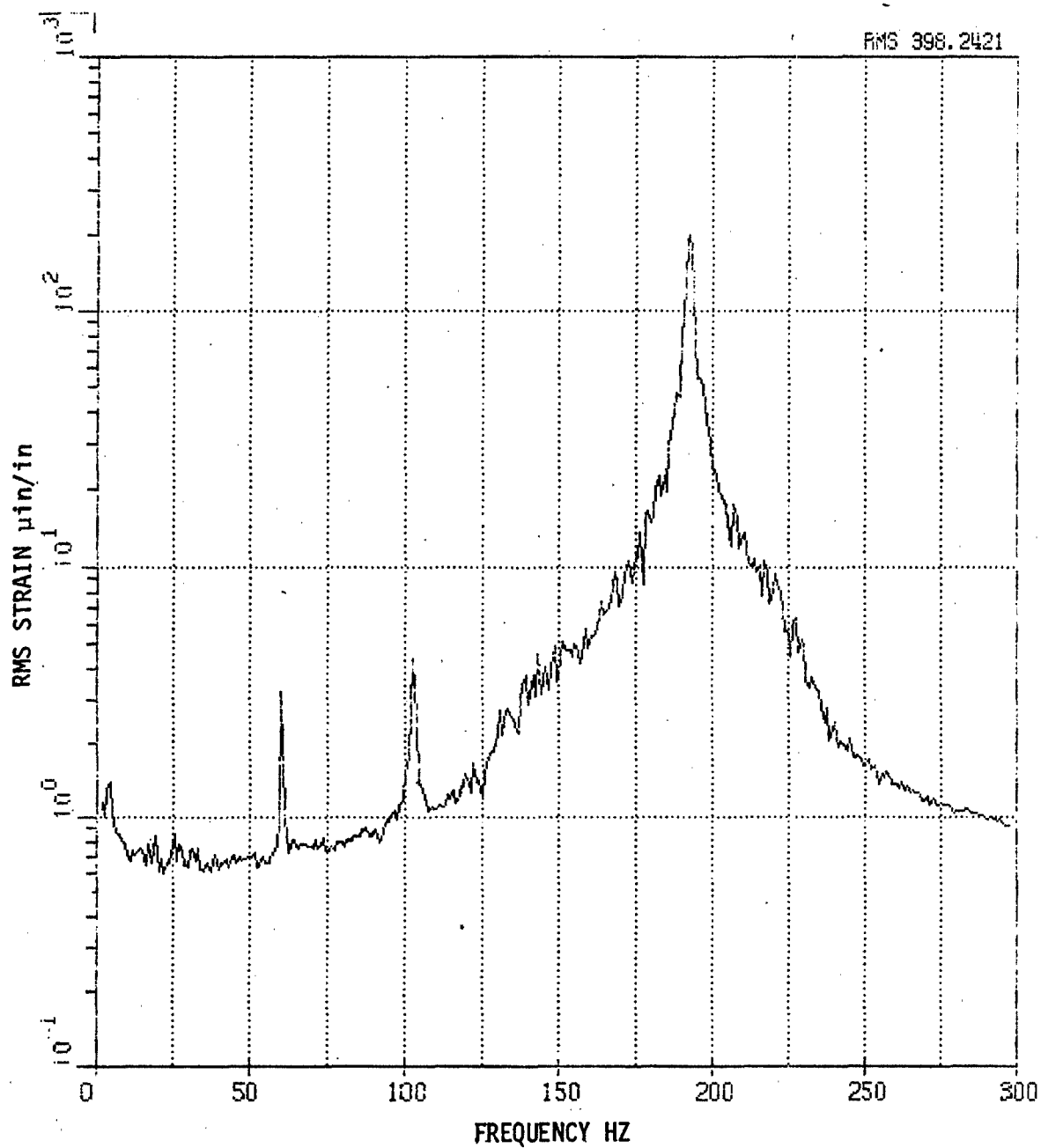


Figure 10. Strain Spectrum on Straingage No. 1, Beam #12, Immediately After Failure.

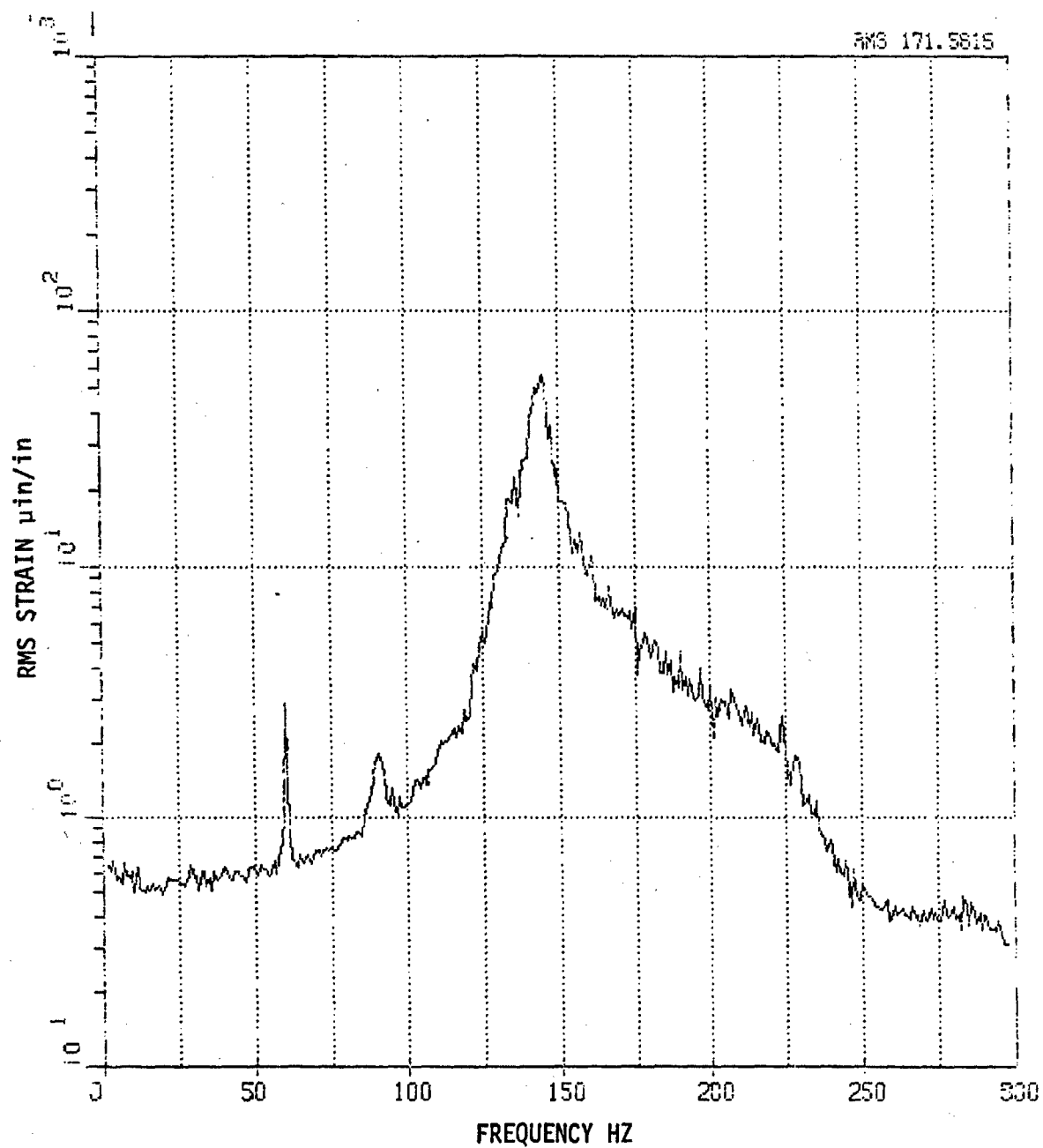


Figure 11. Strain Spectrum on Straingage No. 1, Beam #12, After Crack Propagation to Inner Face Sheet.

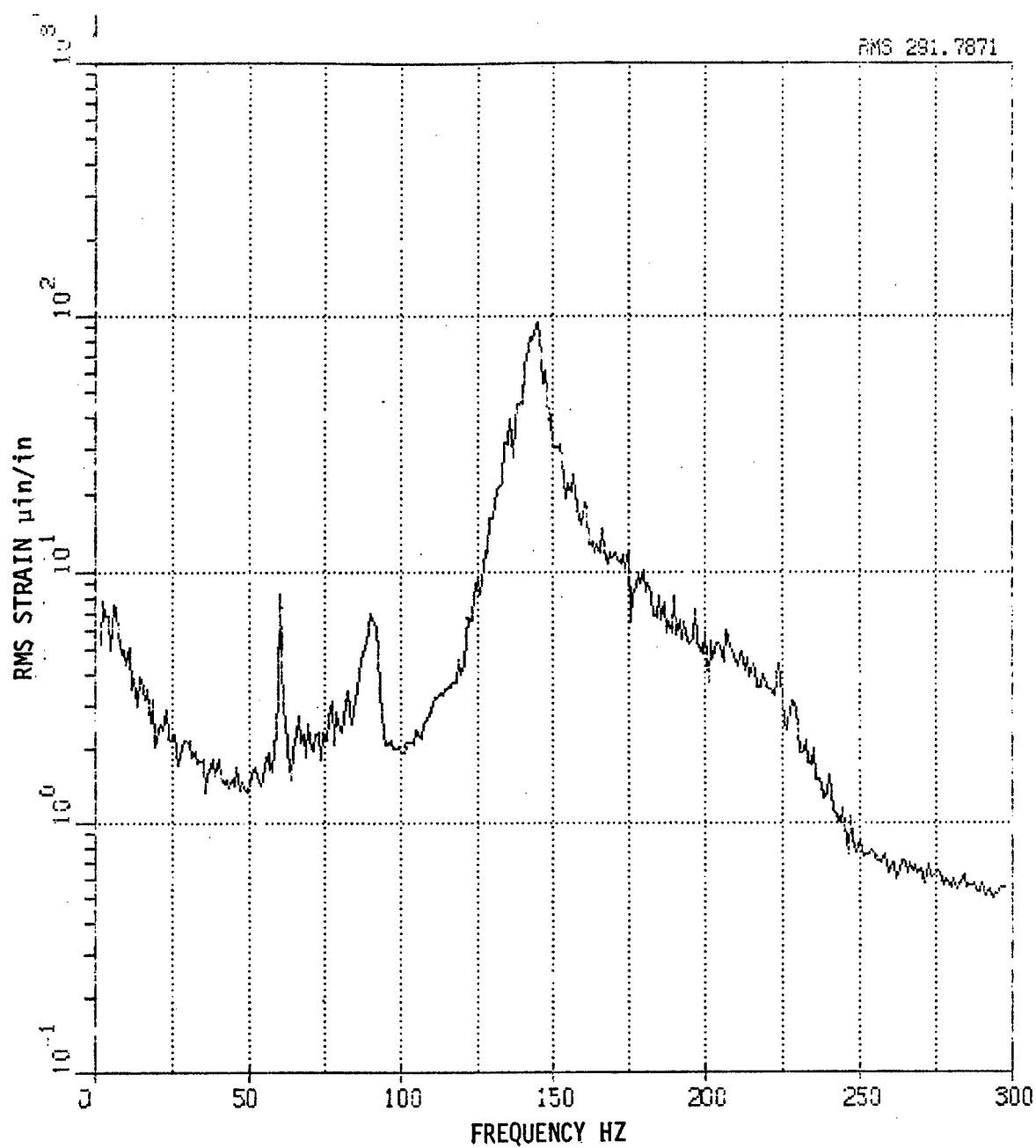


Figure 12. Strain Spectrum on Straingage No. 2, Beam #12, After Crack Propagation to Inner Face Sheet.

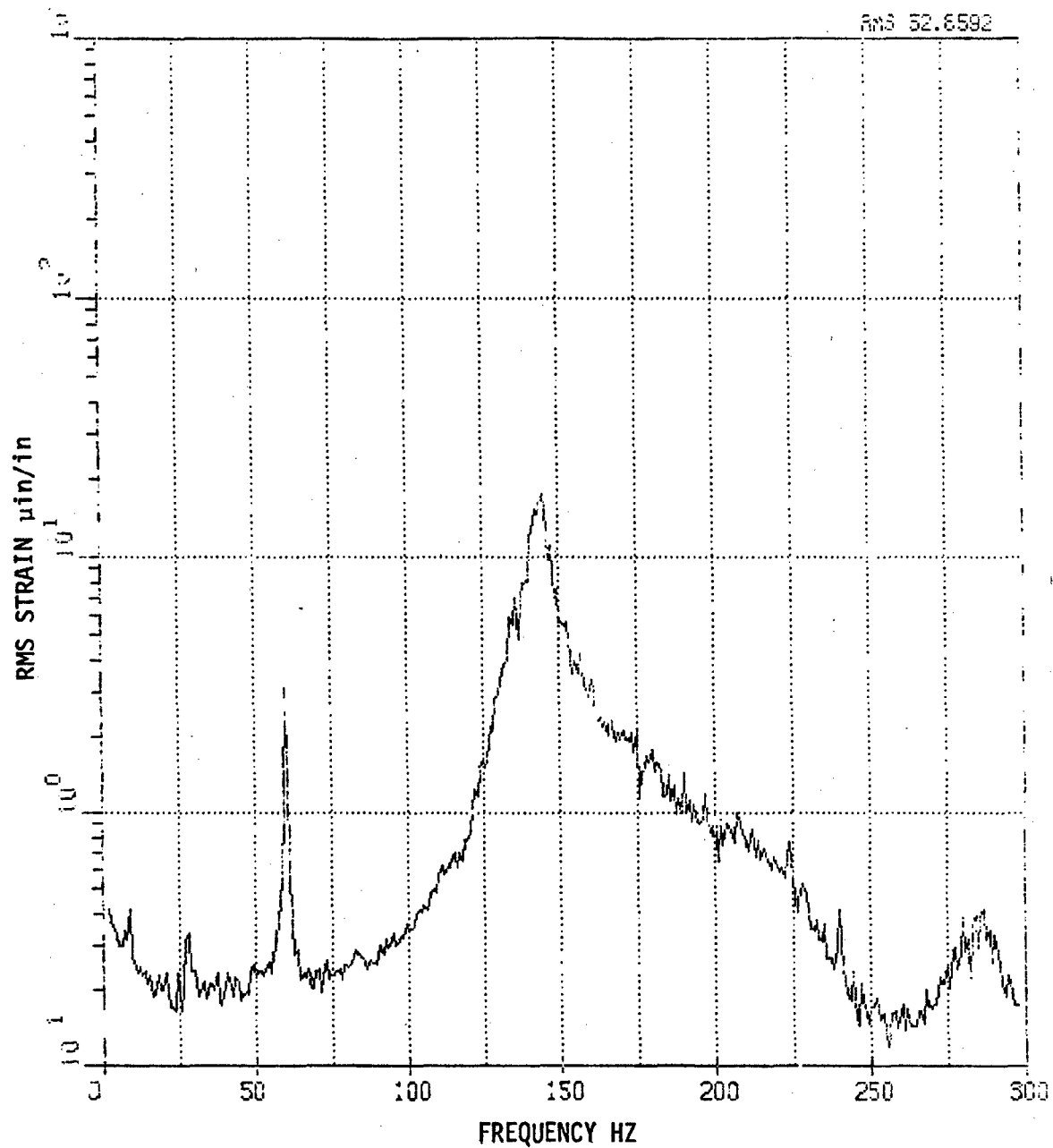


Figure 13. Strain Spectrum on Straingage No. 3, Beam #12, After Crack Propagation to Inner Face Sheet.

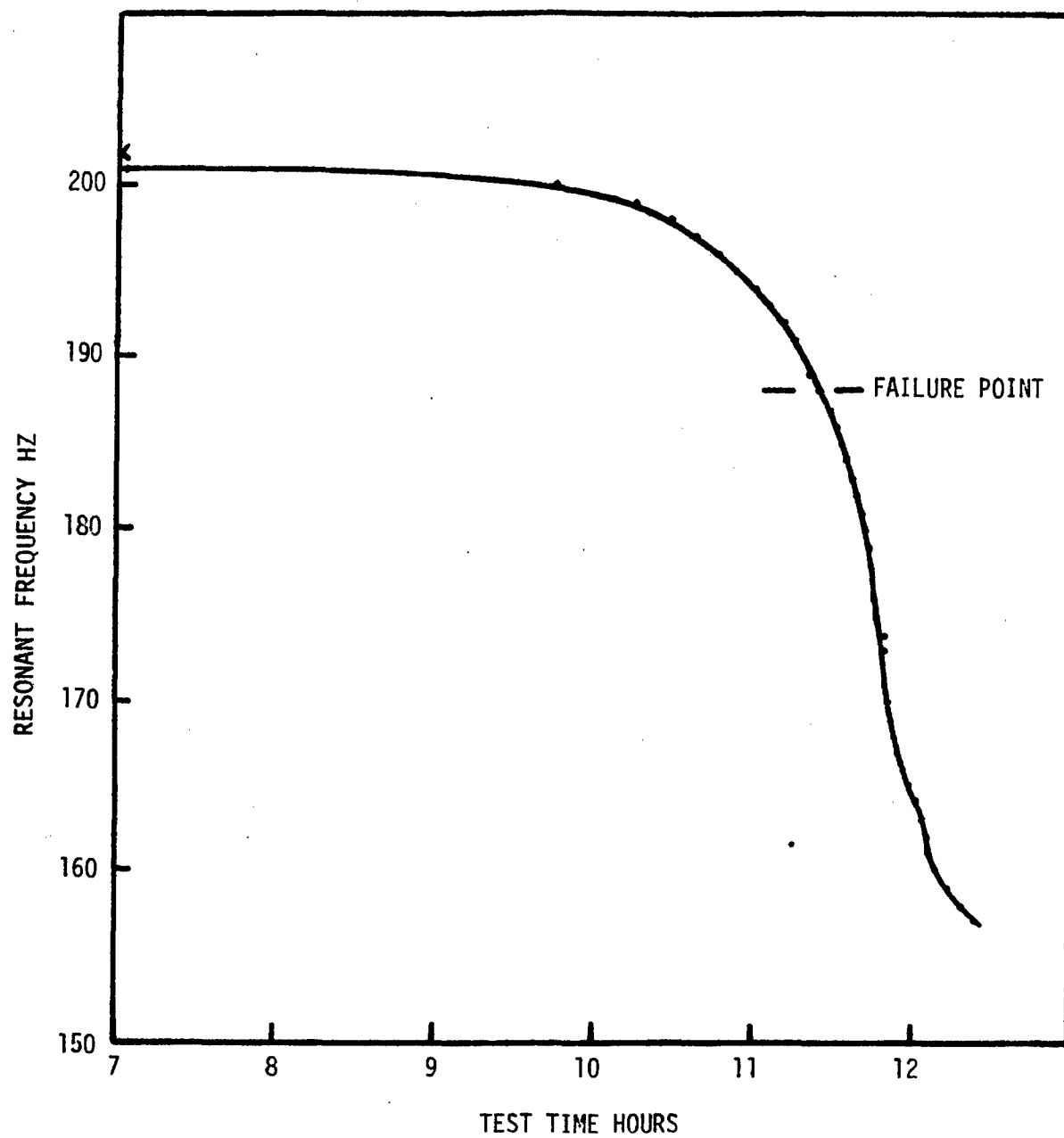


Figure 14. Resonant Frequency Reduction of Testbeam #6.

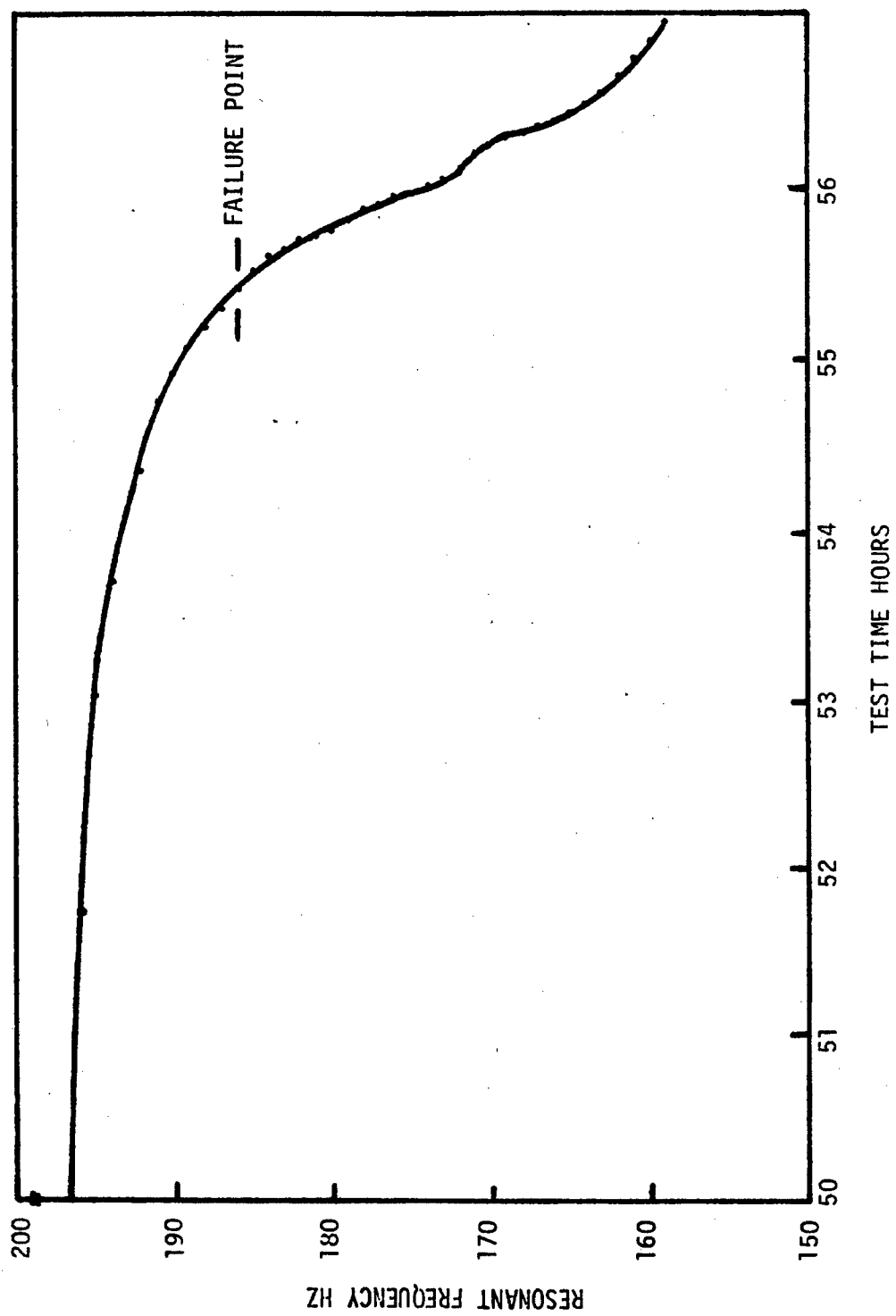


Figure 15. Resonant Frequency Reduction of Testbeam #8.

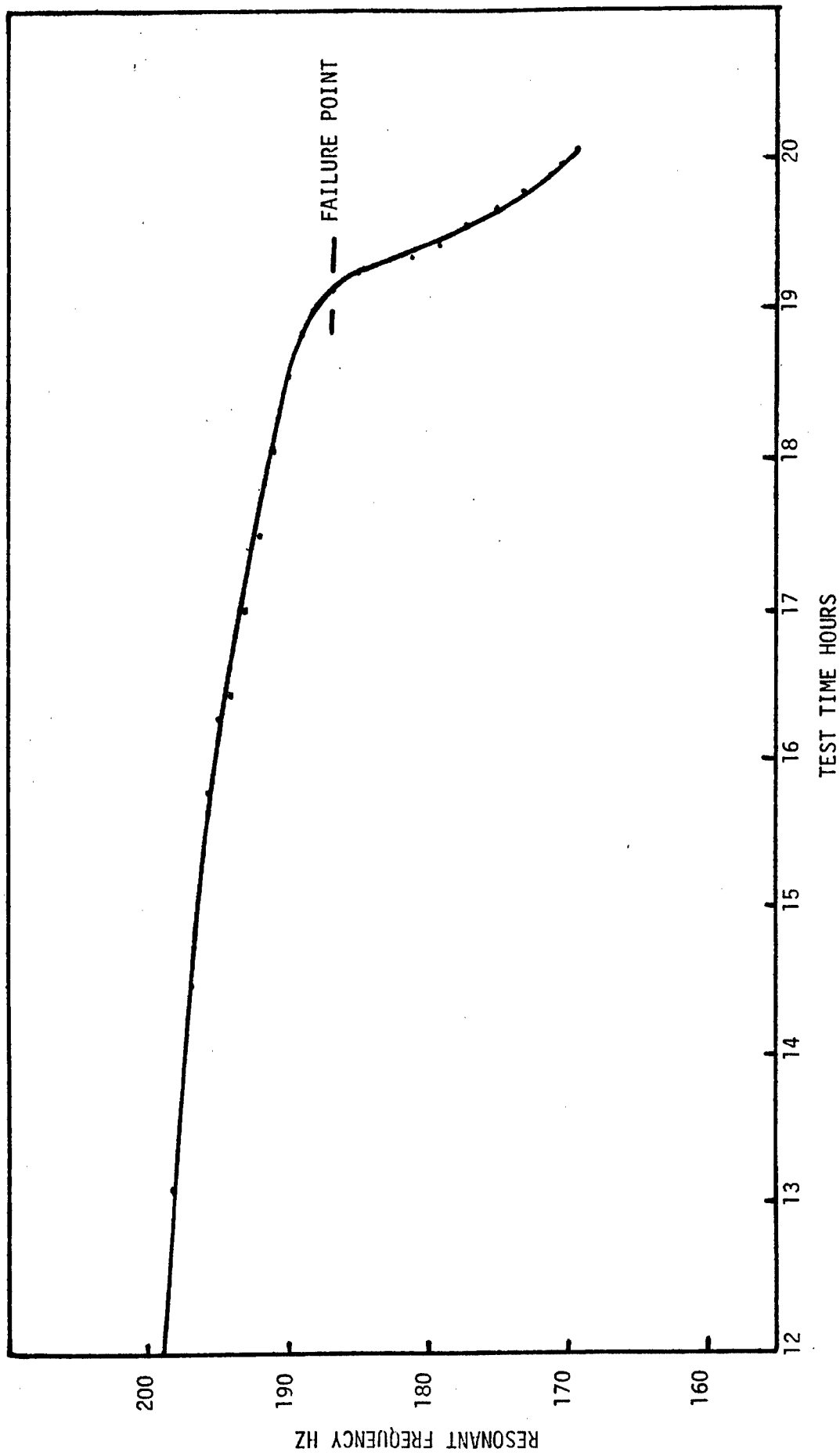


Figure 16. Resonant Frequency Reduction of Testbeam #9.

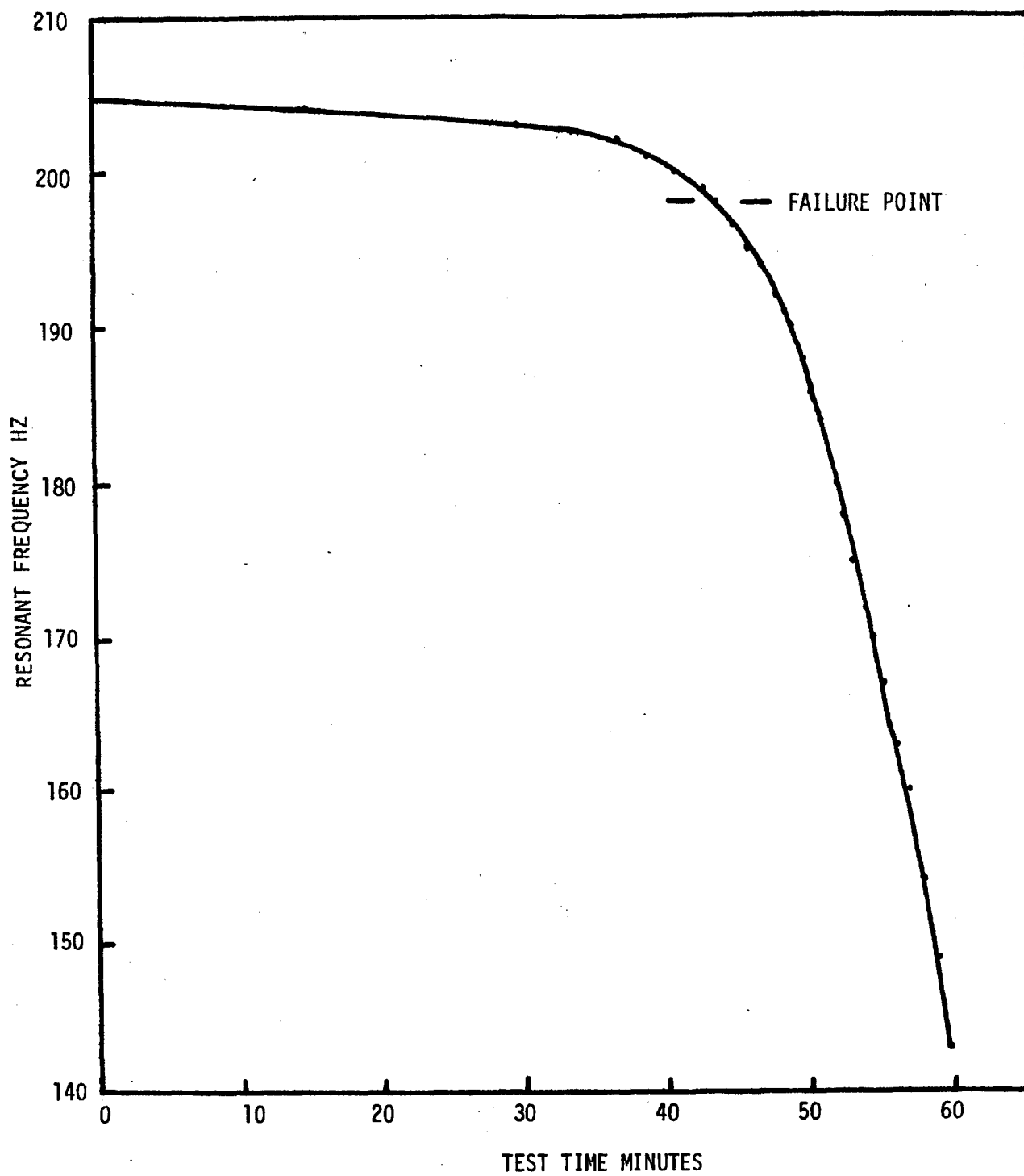


Figure 17. Resonant Frequency Reduction of Testbeam #12.

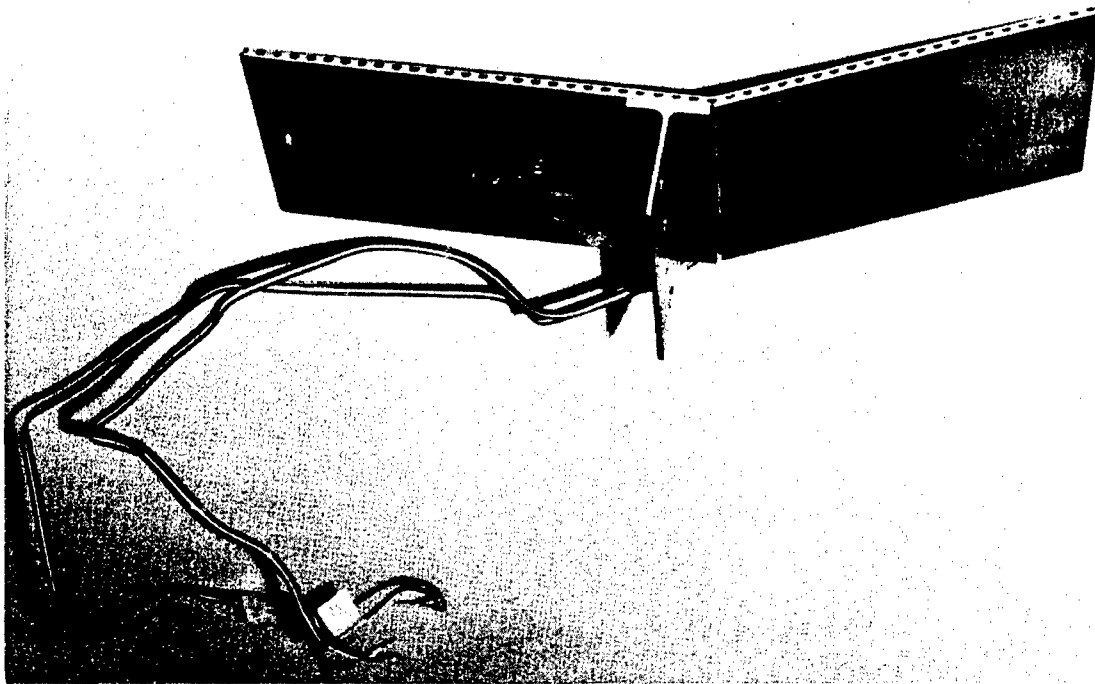
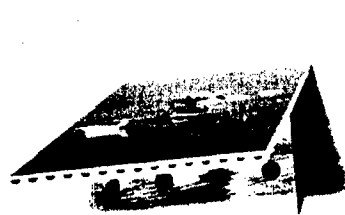
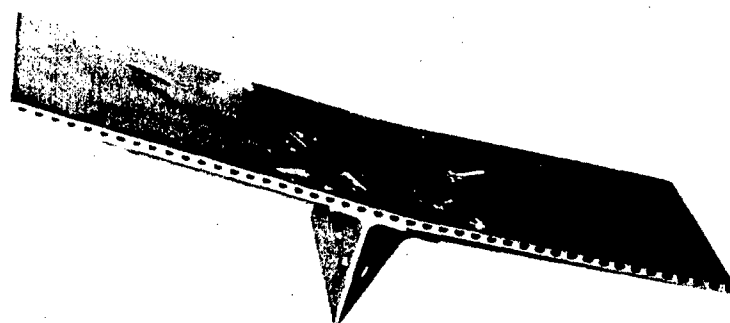


Figure 18. Test Article After Failure. Inner Face Sheet Undamaged.



LONGITUDINAL SLOTS



LATERAL SLOTS

Figure 19. Testbeams with Lateral and Longitudinal Slots.

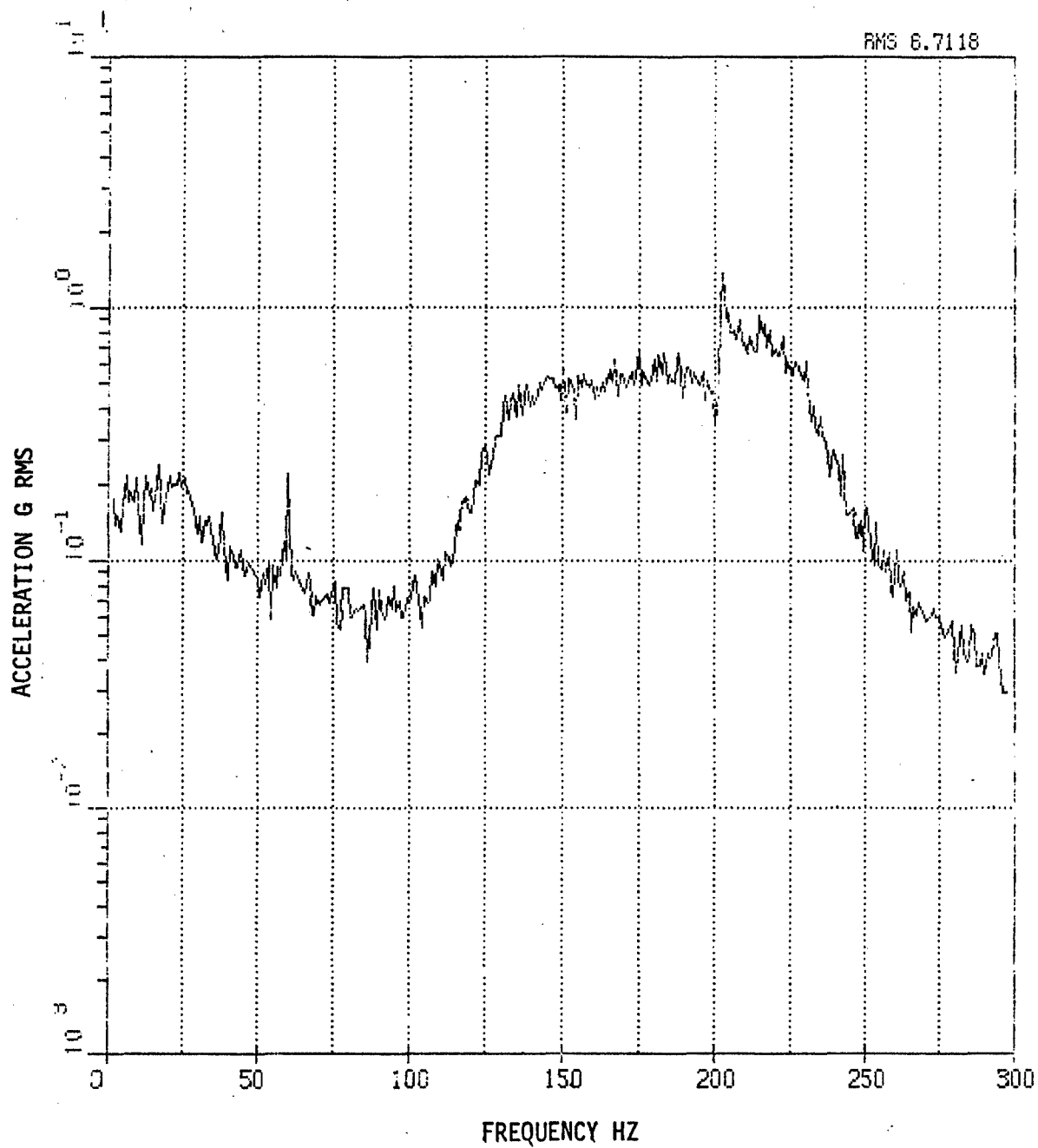


Figure 20. Shaker Excitation Spectrum for Beam #12 Before Failure.

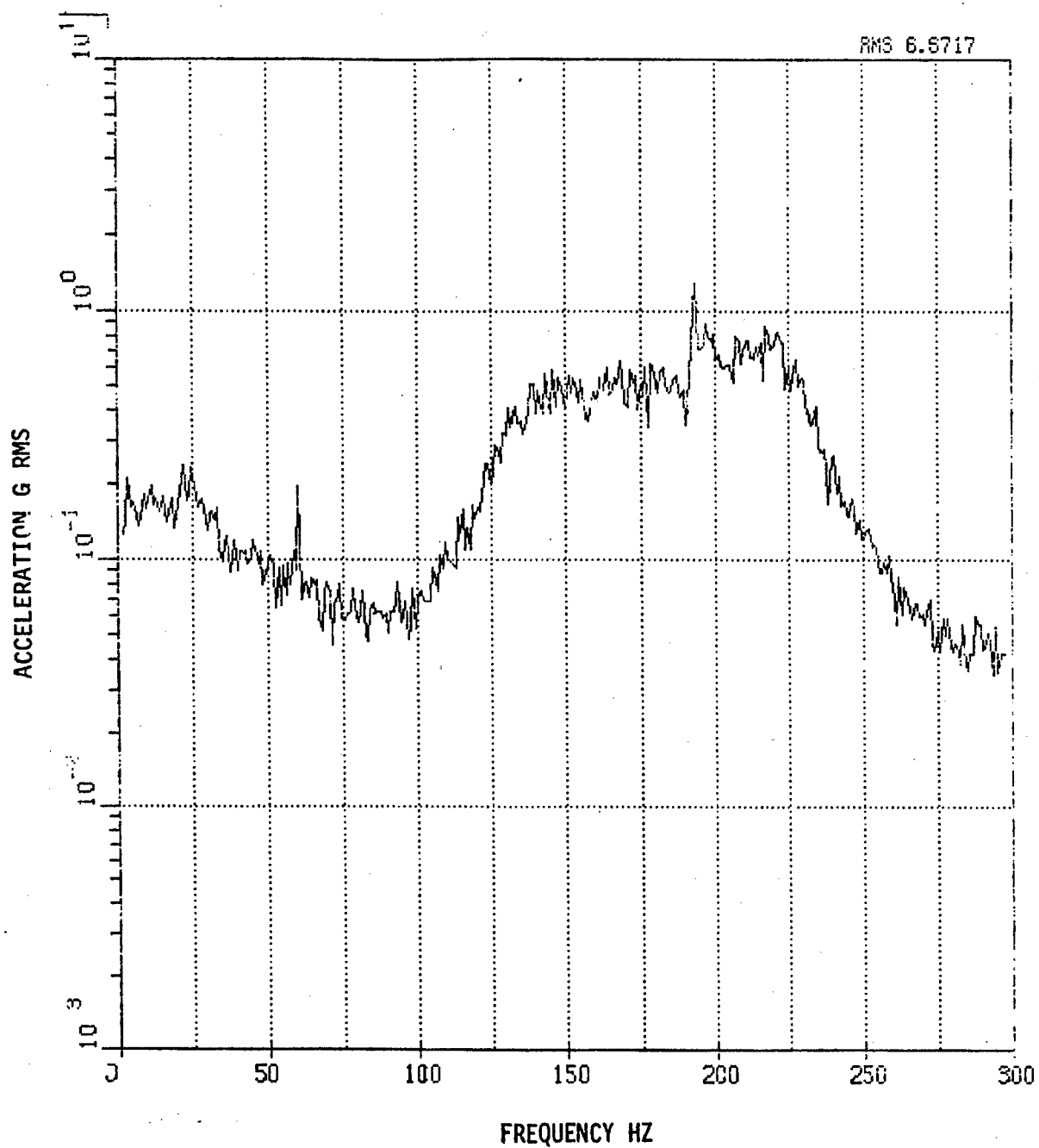


Figure 21. Shaker Excitation Spectrum for Beam #12 After Failure.

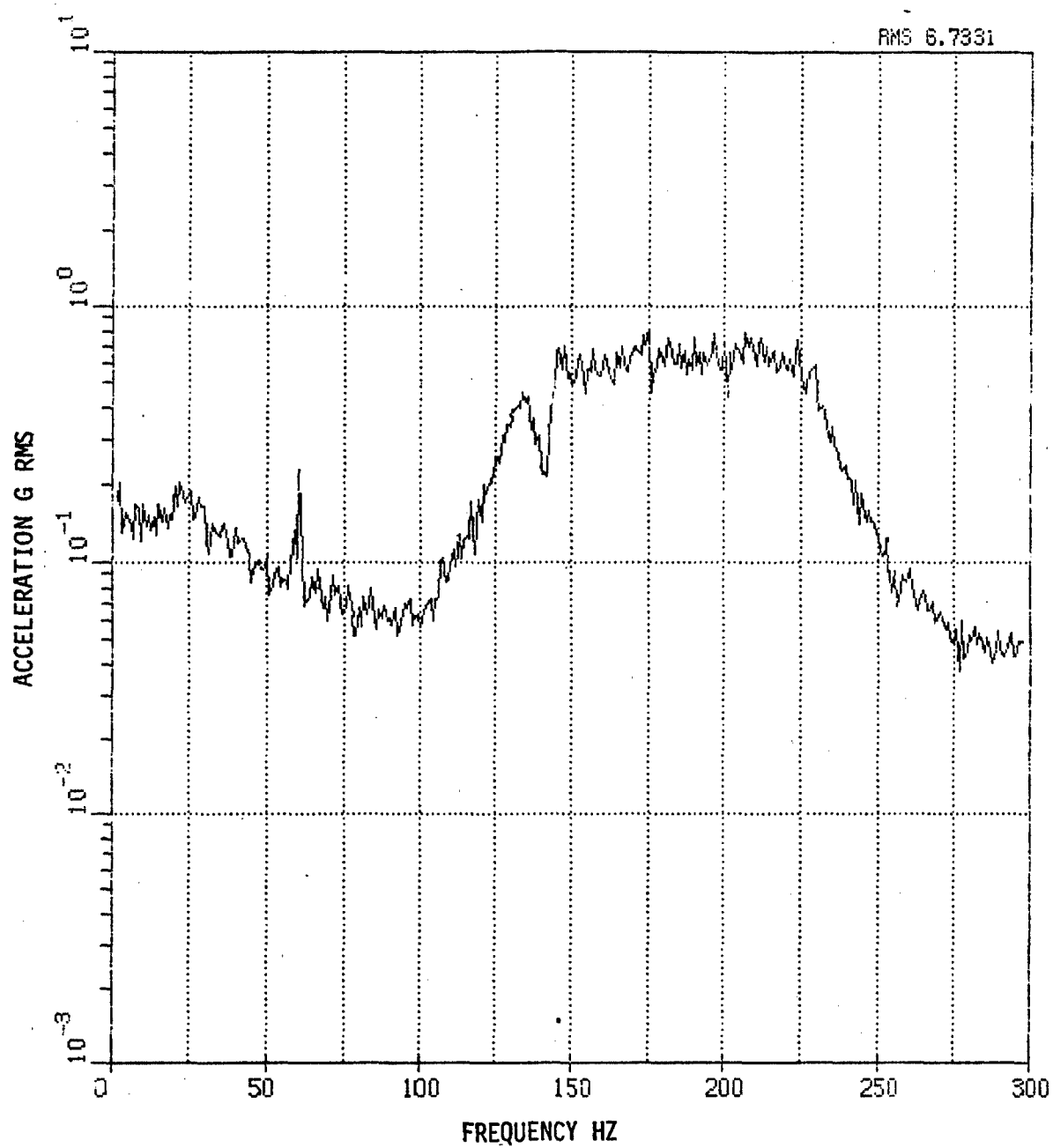


Figure 22. Shaker Excitation Spectrum for Beam #12 After Crack Propagation Through Outer Face Sheet.

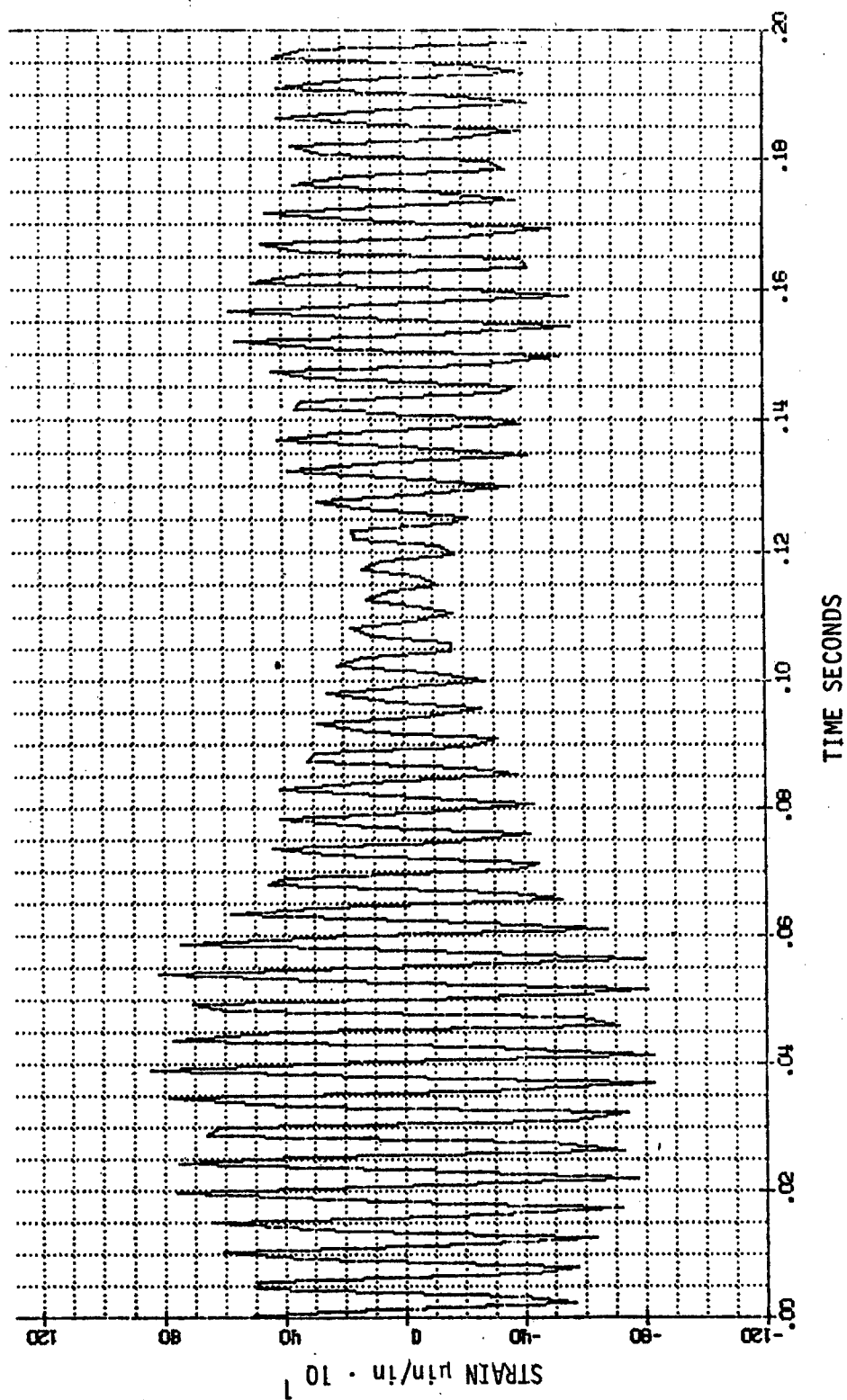


Figure 23. Section of Strain Time History of Beam #2.

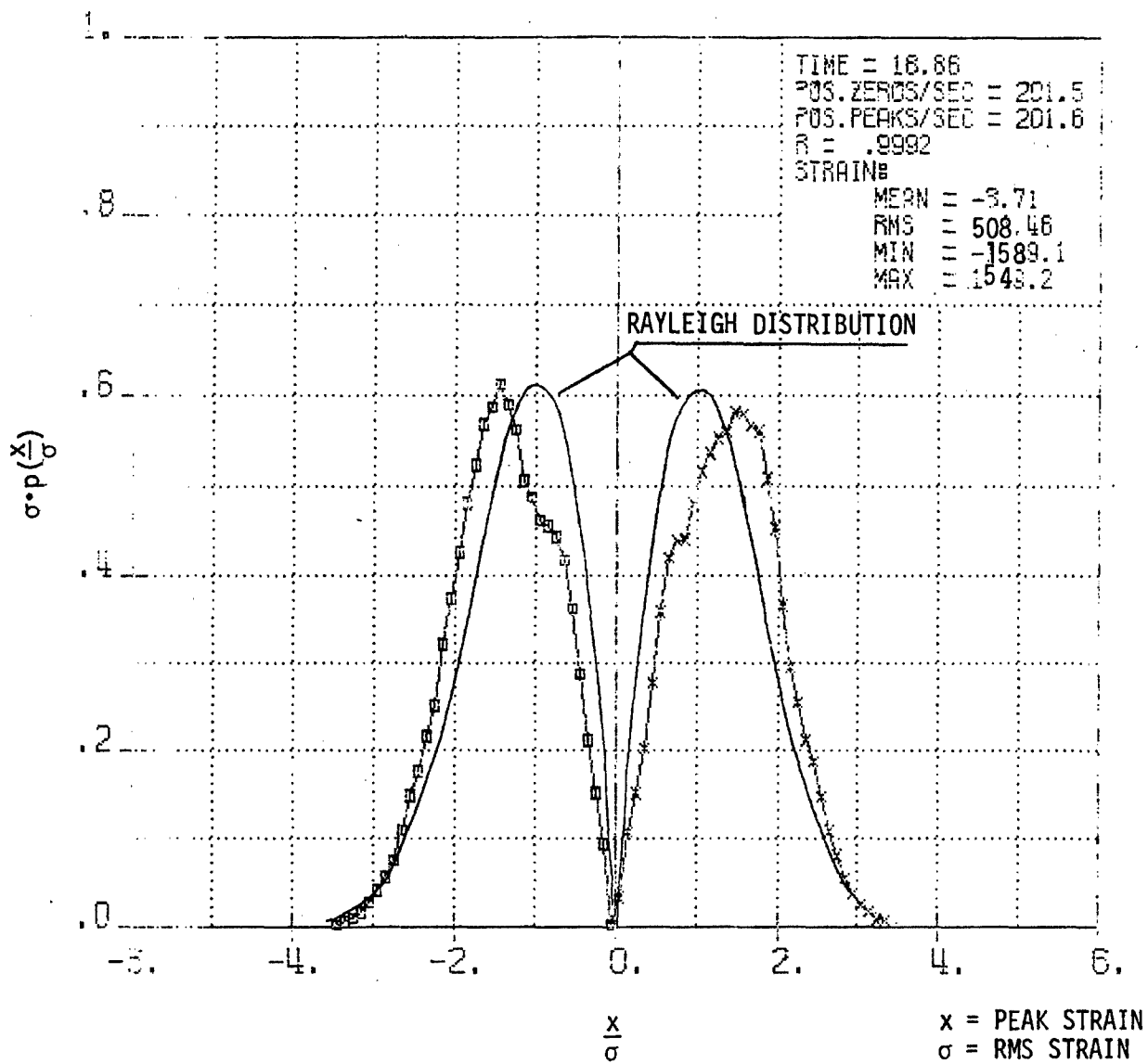


Figure 24. Strain Peak Probability Density on Testbeam #12 Before Failure.

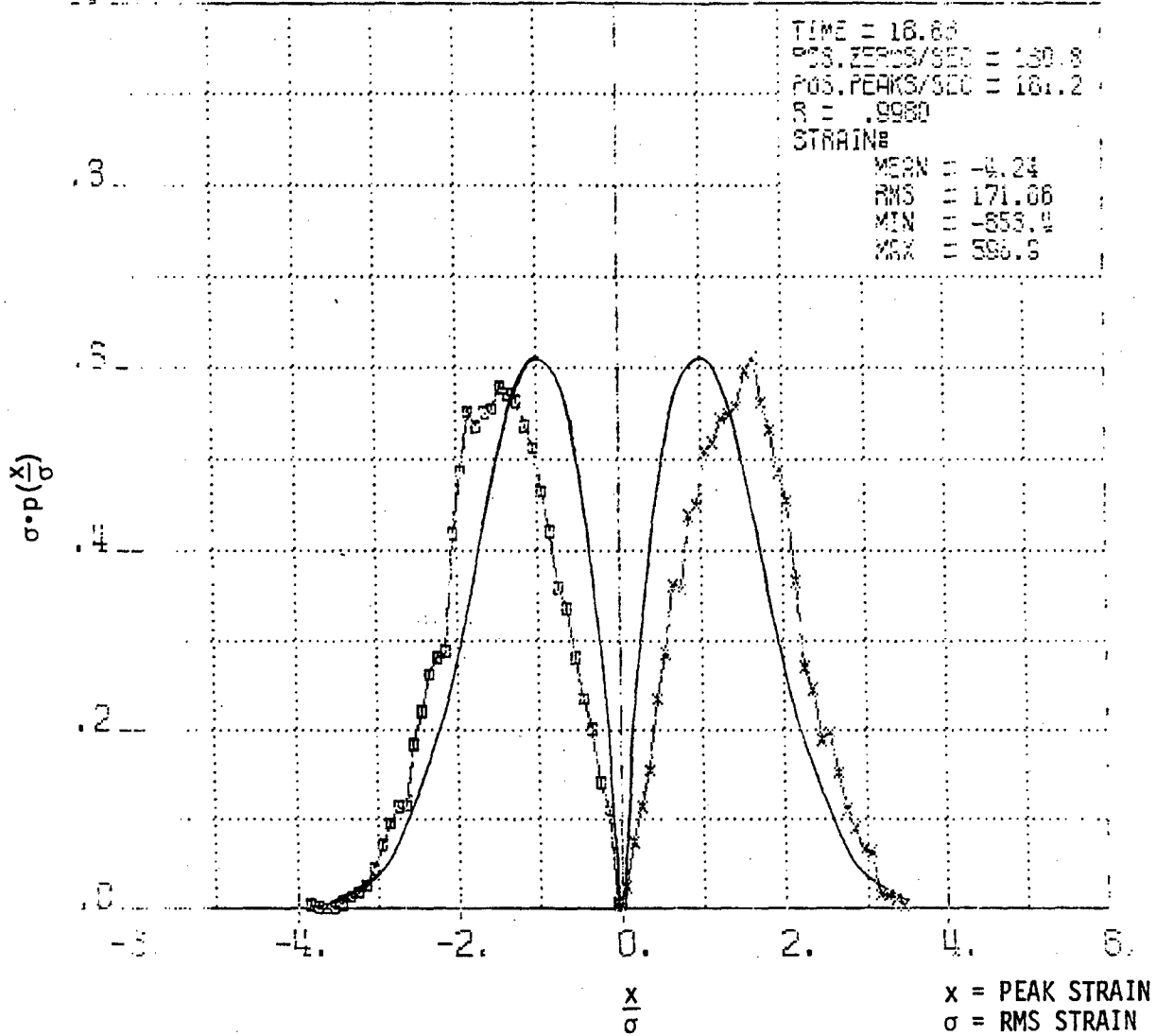


Figure 25. Strain Peak Probability Density on Testbeam #12 After Failure.

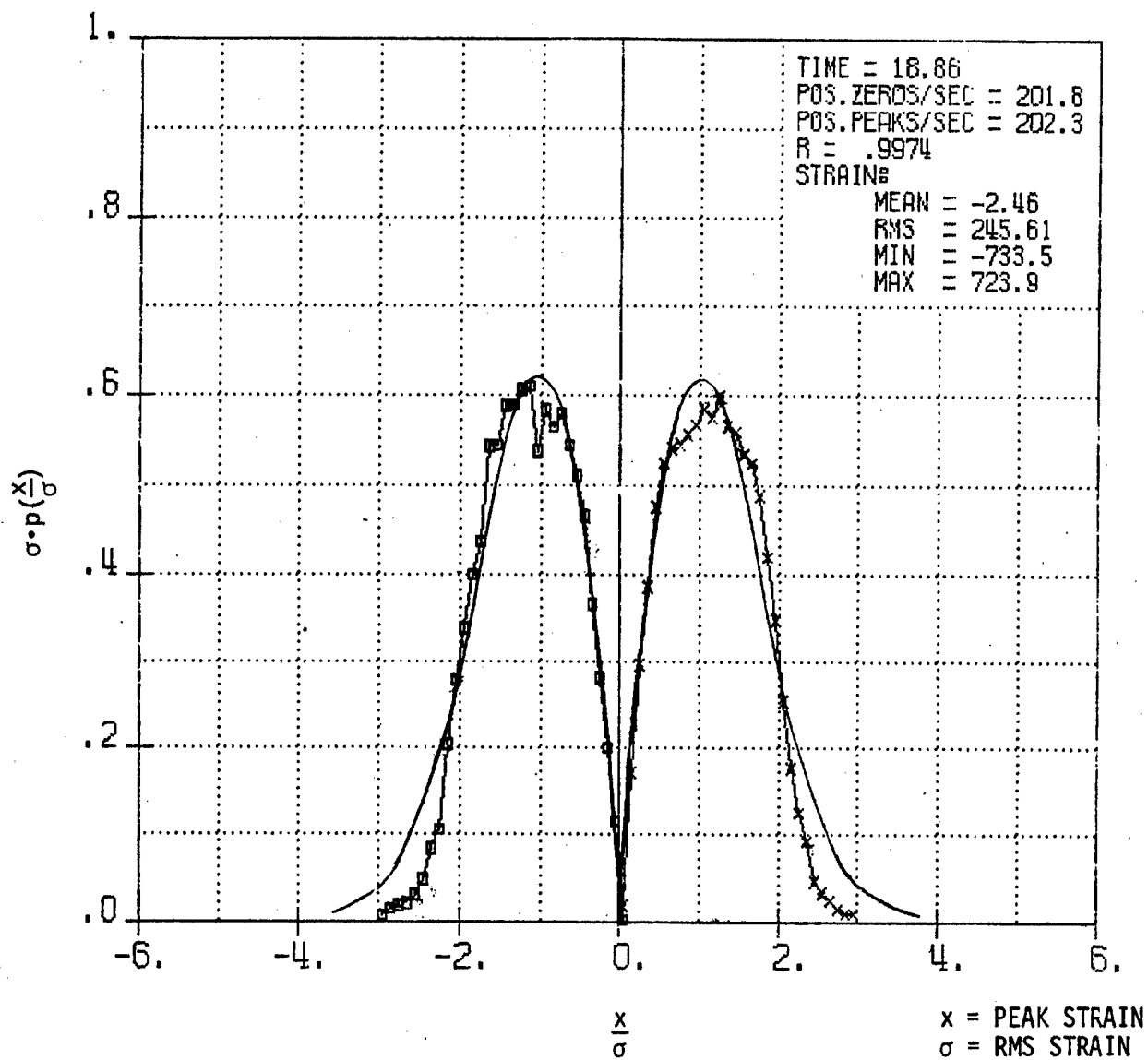


Figure 26. Strain Peak Probability Density on Testbeam #11 Before Failure.

AISI-347

$$\epsilon_{rms_1} = 3.518 \times 10^3 N^{-.1483}$$

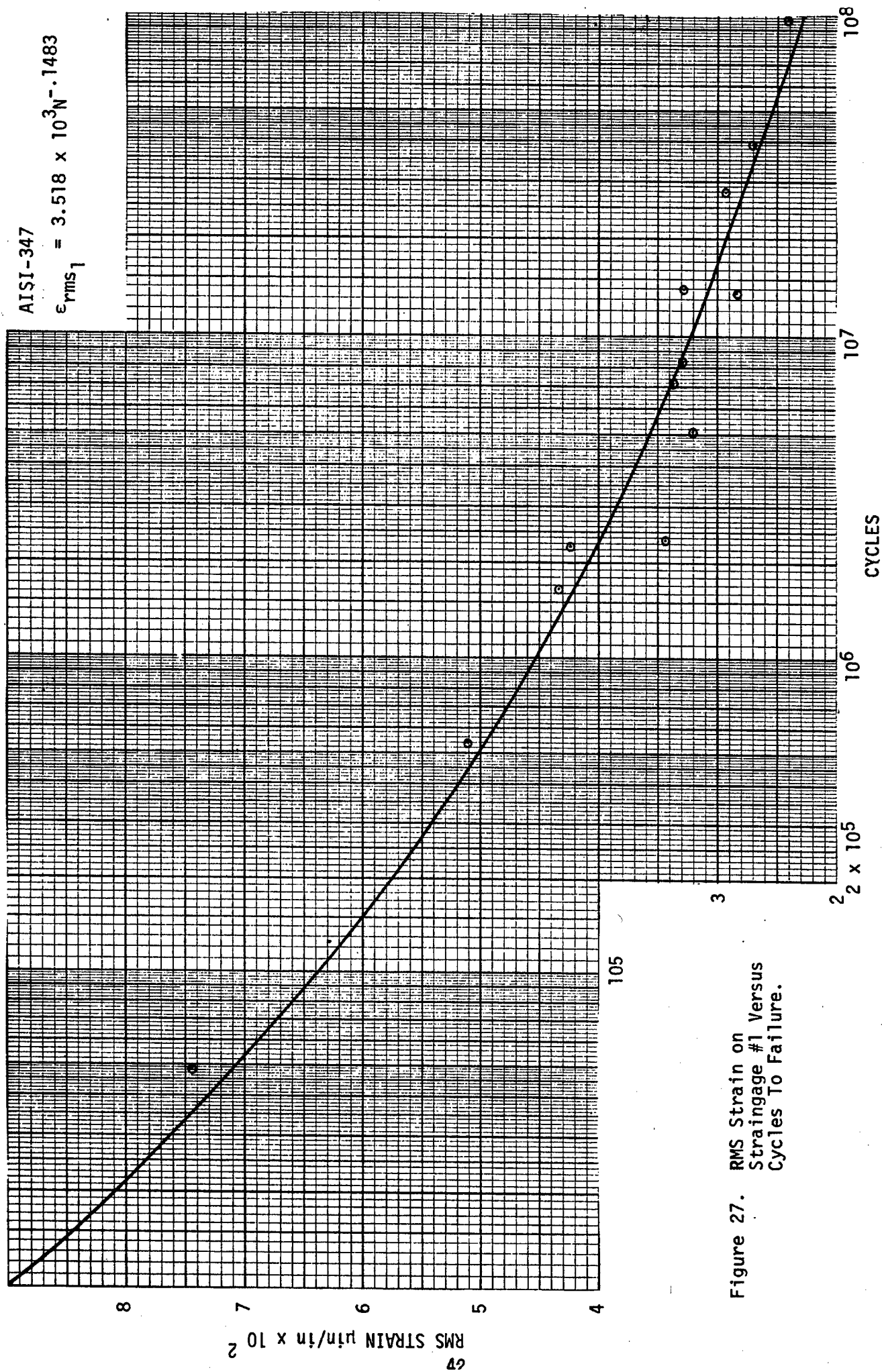


Figure 27. RMS Strain on Strainage #1 Versus Cycles To Failure.

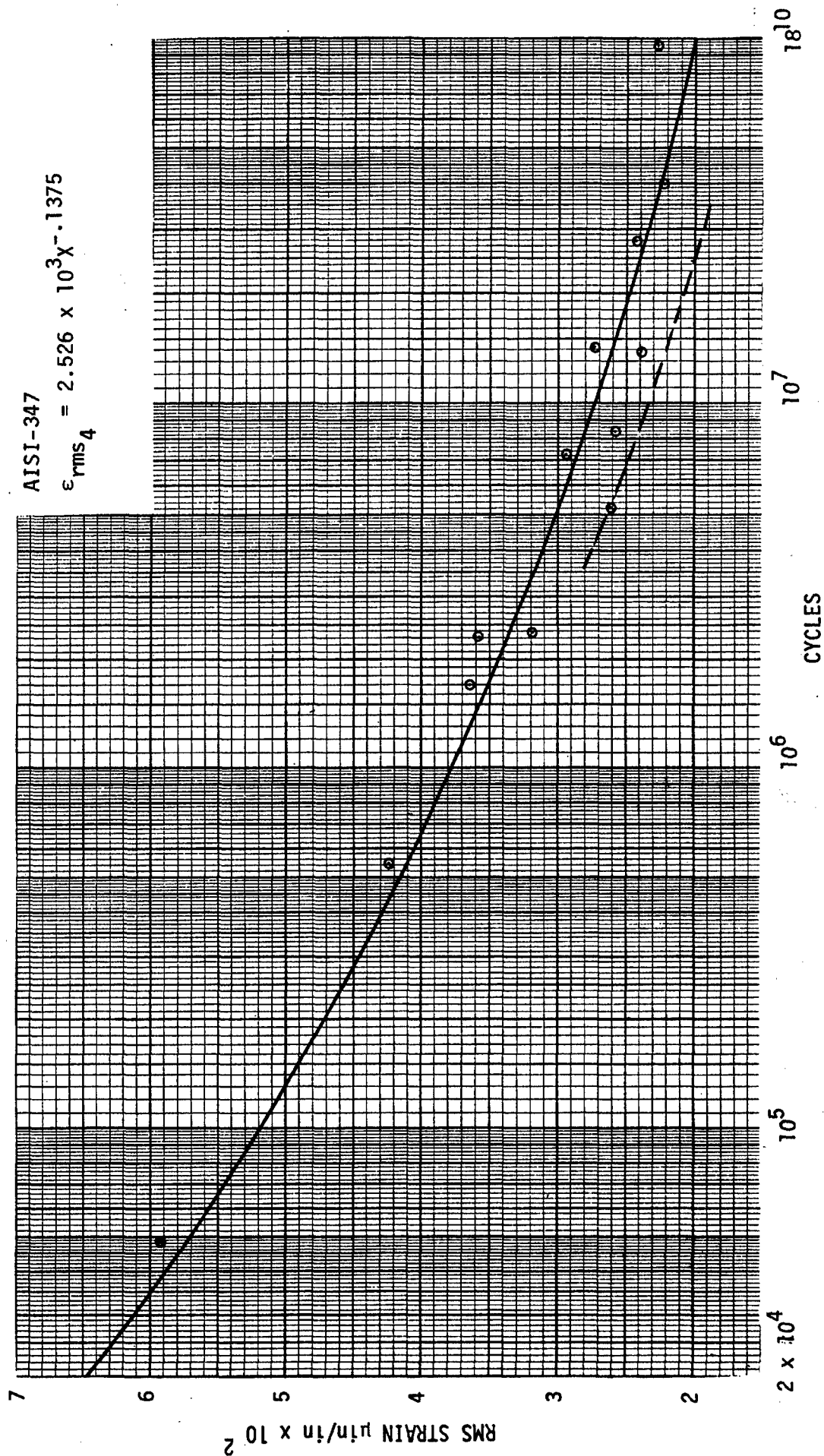


Figure 28. RMS Strain on Strainage #4 Versus Cycles To Failure.

AISI-347

$$S_{rms_1} = 9.861 \times 10^4 N^{-.1484}$$

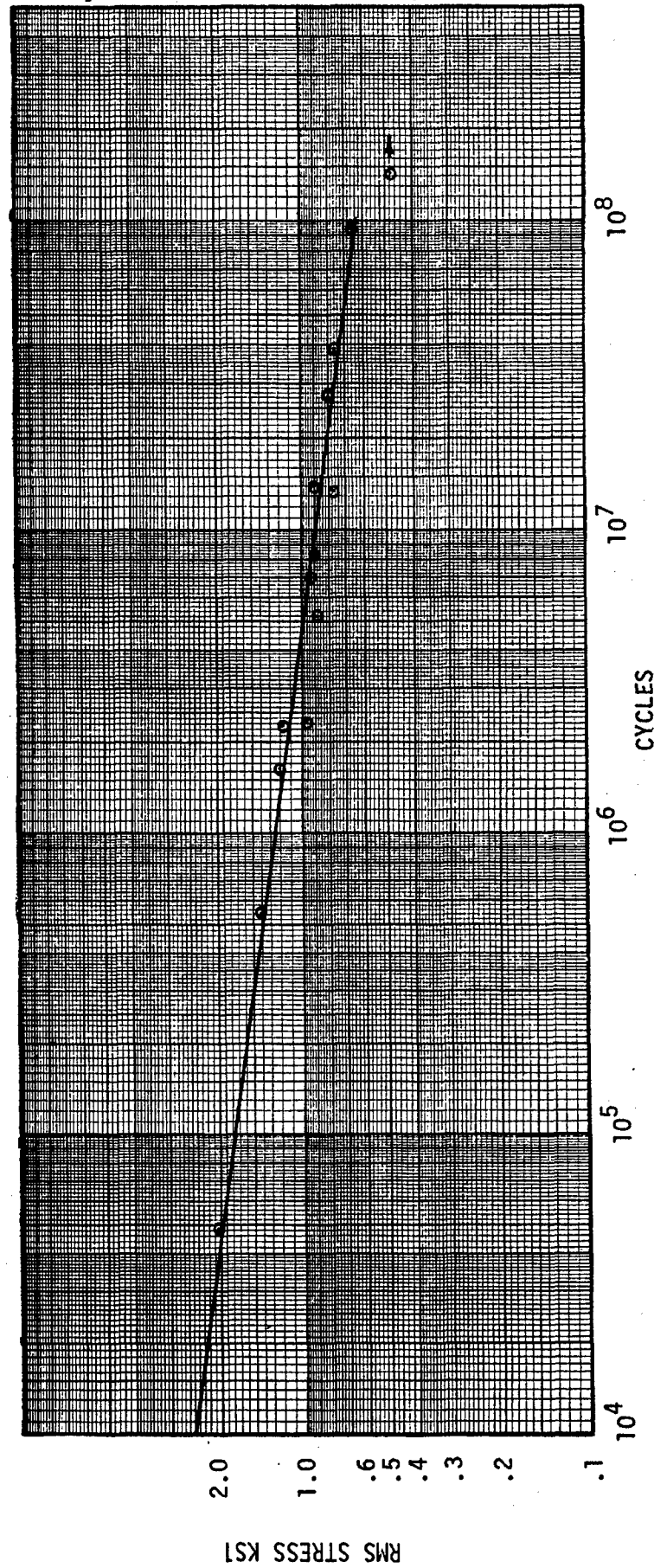


Figure 29. RMS Stress Versus Cycles to Failure as Measured on Strainage #1.

AISI-347

$$S_{rms_1} = 7.073 \times 10^6 N^{-.1375}$$

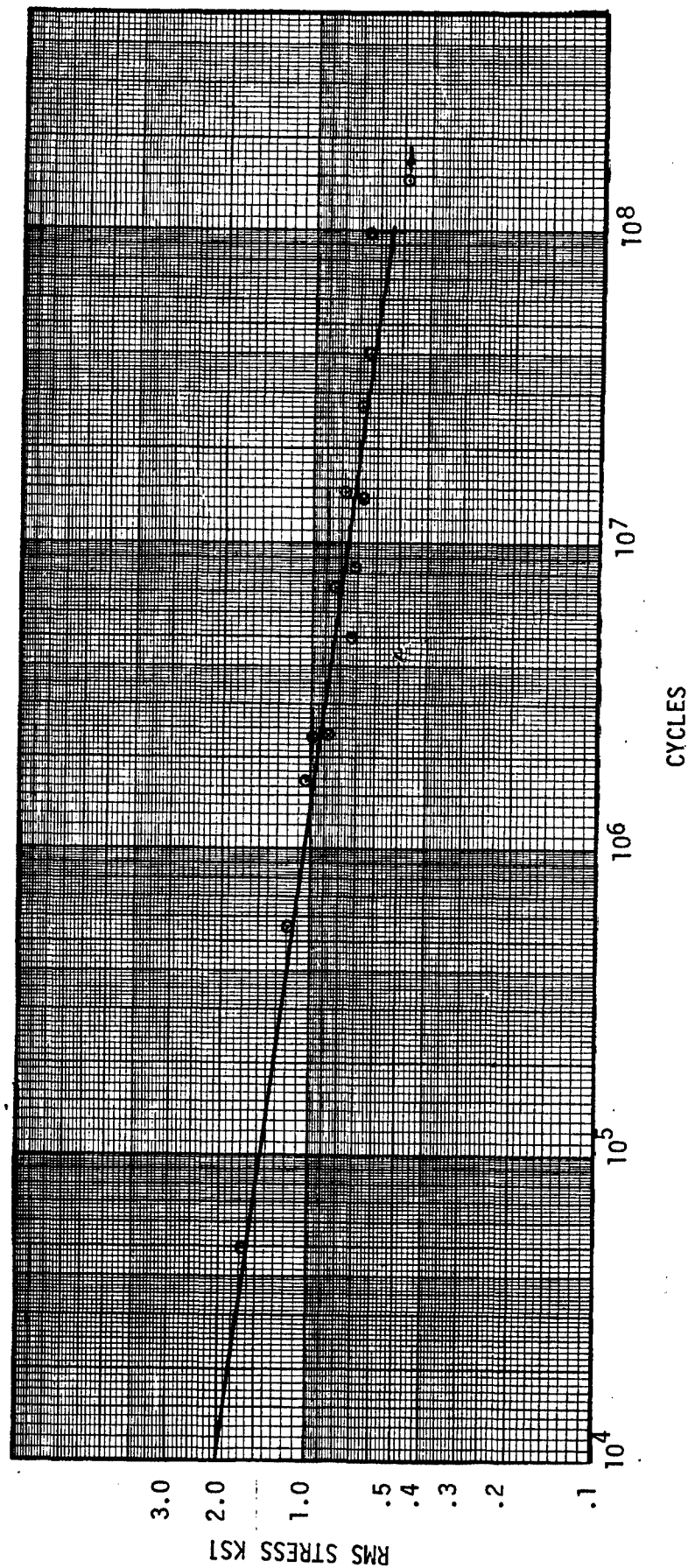


Figure 30. RMS Stress Versus Cycles to Failure as Measured on Strainage #4.

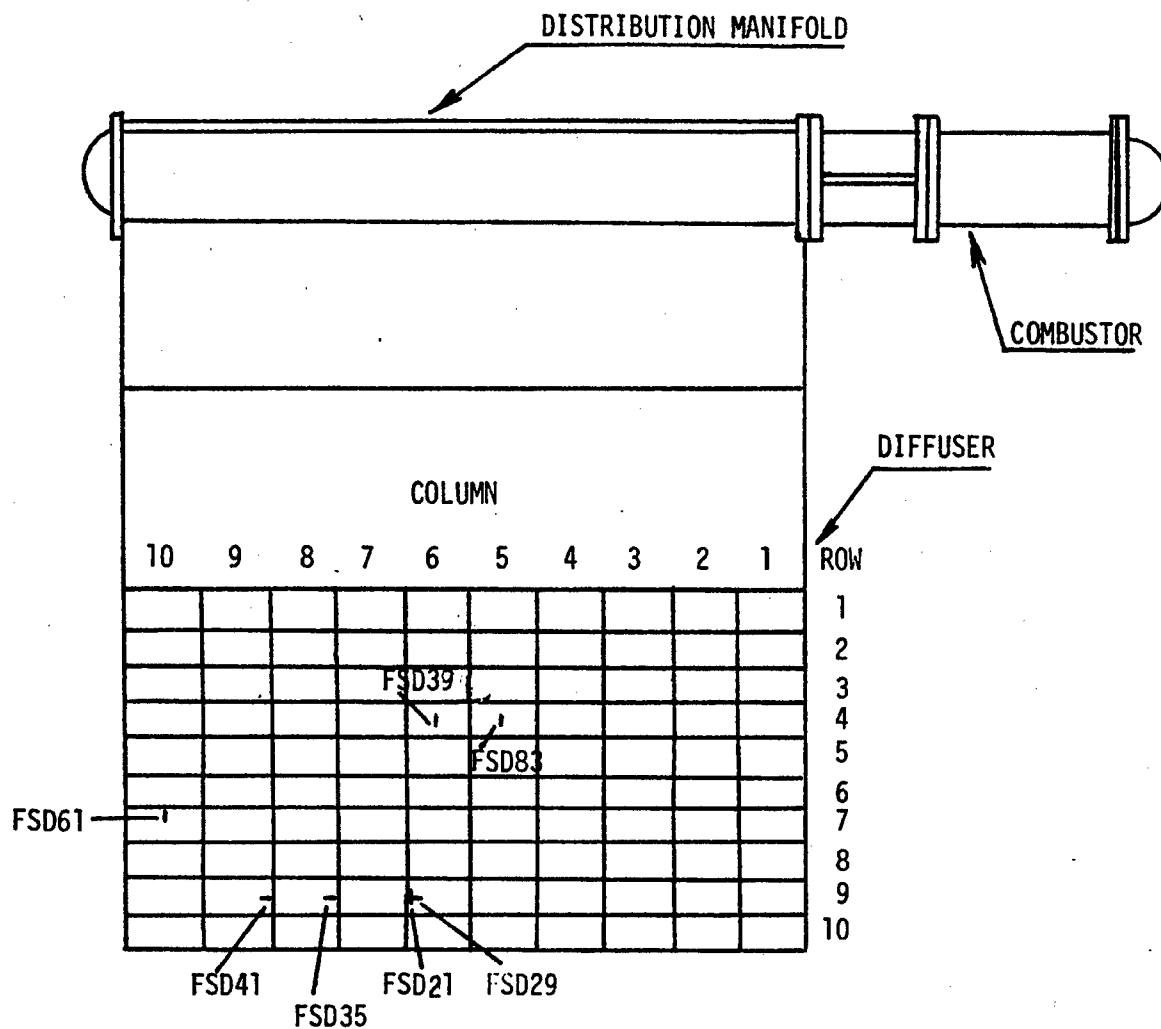


Figure 31. GDL Right Hand Stage, Inboard Diffuser Sidewall, Straining Locations.

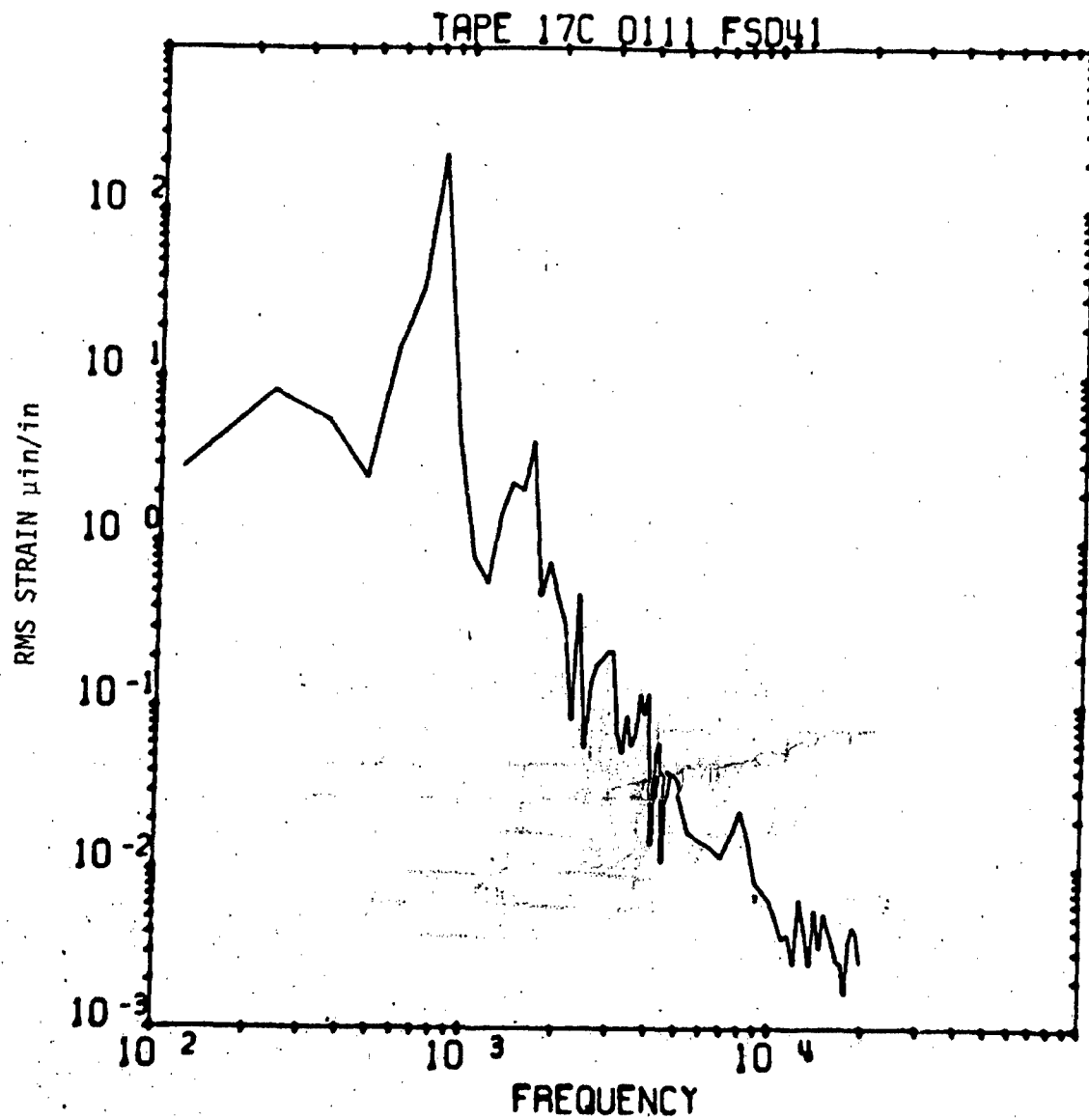


Figure 32. Strain Spectrum on Straingage FSD 41 During GDL Run 111.

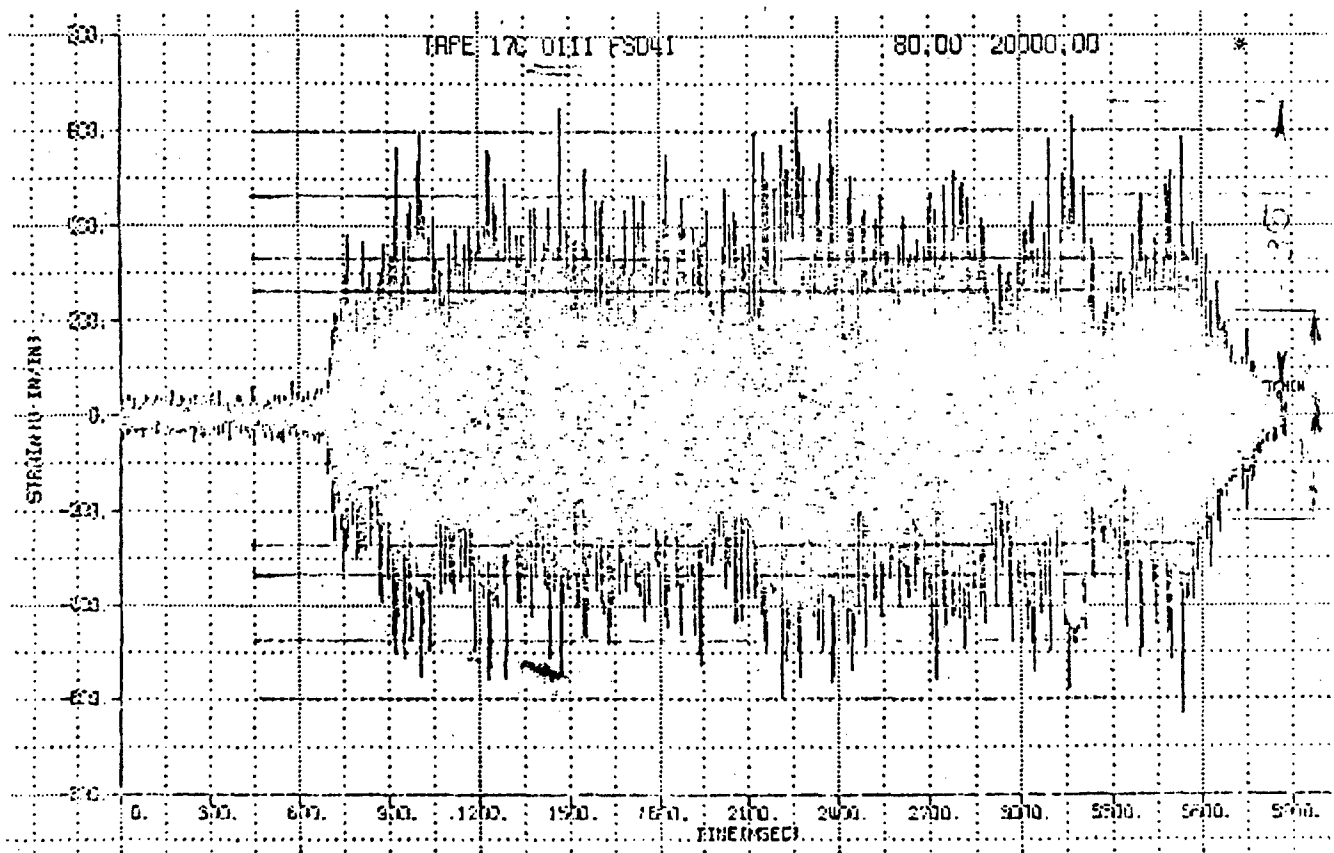


Figure 33. Strain Time History of GDL Run 111 on Strainage FSD 41.

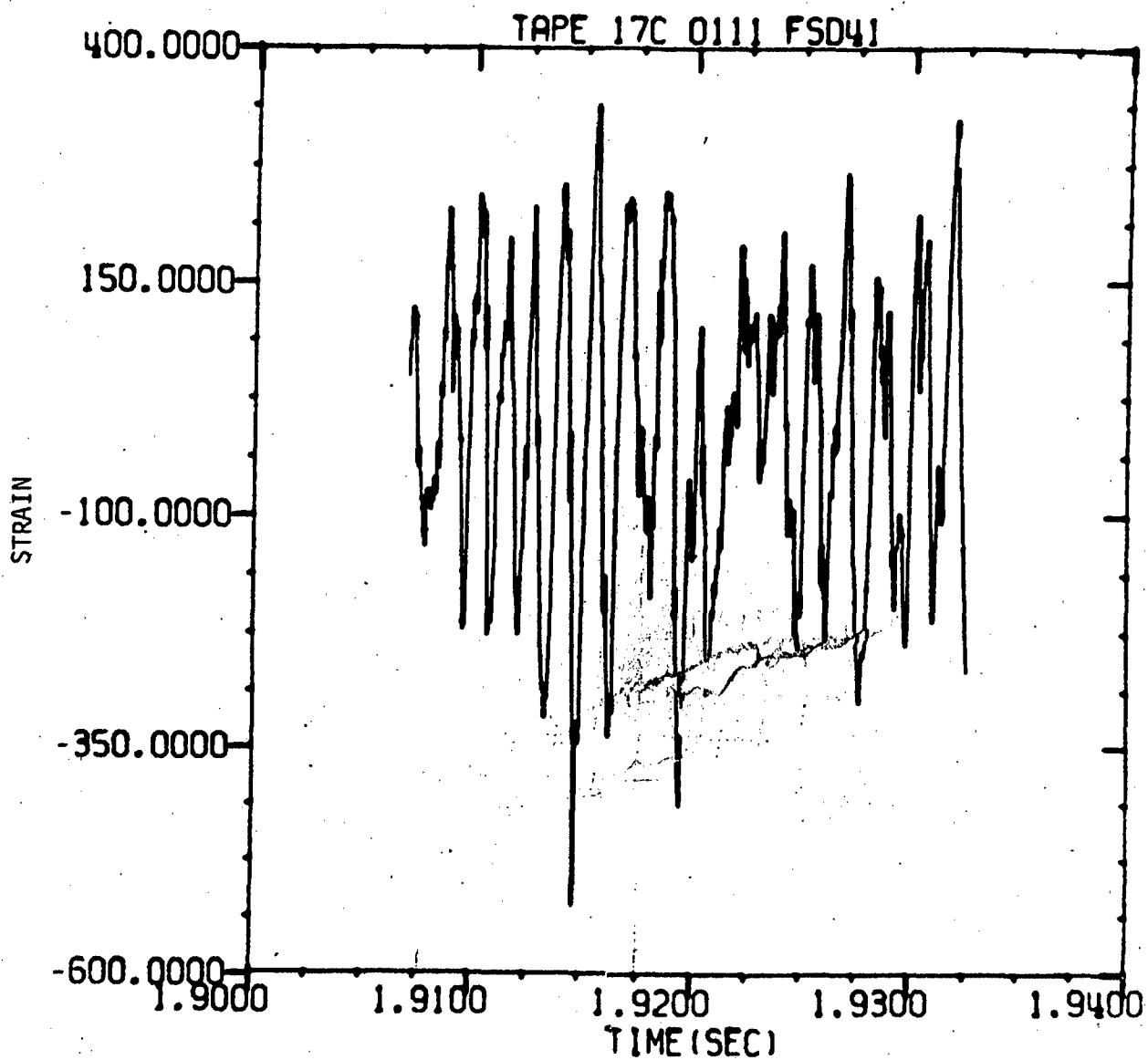


Figure 34. Section of Strain Time History on Strainage FSD 41
During GDL Run 111.